Lagrangian fillings in A-type and their Kálmán loop orbits

James Hughes

Abstract. We compare two constructions of exact Lagrangian fillings of Legendrian positive braid closures, the Legendrian weaves of Casals–Zaslow, and the decomposable Lagrangian fillings of Ekholm–Honda–Kálmán, and show that they coincide for large families of Lagrangian fillings. As a corollary, we obtain an explicit correspondence between Hamiltonian isotopy classes of decomposable Lagrangian fillings of Legendrian $(2, n)$ torus links described by Ekholm–Honda–Kálmán and the weave fillings constructed by Treumann and Zaslow. We apply this result to describe the orbital structure of the Kálmán loop and give a combinatorial criteria to determine the orbit size of a filling. We follow our geometric discussion with a Floer-theoretic proof of the orbital structure, where an identity studied by Euler in the context of continued fractions makes a surprise appearance. We conclude by giving a purely combinatorial description of the Kálmán loop action on the fillings discussed above in terms of edge flips of triangulations.

1. Introduction

Legendrian links and their exact Lagrangian fillings are objects of interest in contact and symplectic topology [4, 12, 16, 17]. Within the last decade, parallel developments in the constructive methods [11, 15] and the application of both Floer-theoretic [9, 23, 30] and microlocal-sheaf-theoretic [6, 36, 37] invariants have significantly advanced the classification of Lagrangian fillings. Broadly speaking, this manuscript aims to compare the two primary methods of constructing Lagrangian fillings, [11] and [15], of Legendrian positive braid closures. We then leverage this result in the well-studied case of Lagrangian fillings of Legendrian $(2, n)$ torus links in the standard contact 3-sphere to understand the action of a Legendrian loop on these fillings. In addition to a contact geometric approach, we discuss insights into properties of the augmentation variety associated to this class of Legendrian links afforded by this comparison.

Denote by σ_i the ith Artin generator of the n-stranded braid group Br_n, and let β be a positive braid, i.e., a product of positive powers of σ_i. We define the family of maximal-tb Legendrian links $\lambda(\beta)$ in the front projection as the rainbow closure of β, as depicted in

Figure 1 (left). Legendrian $(2, n)$ torus links are given by the braid $\sigma_1^n \subseteq \mathrm{Br}_2$. They are also smoothly described as the link of the complex A_{n-1}-singularity $f(x, y) = x^n + y^2$, and hence we will also denote Legendrian $(2, n)$ torus links by $\lambda(A_{n-1})$. The Lagrangian fillings that we will consider in this manuscript are all exact, orientable, and embedded in the standard symplectic 4-ball $(\mathbb{D}^4, \lambda_{\mathrm{st}})$, whose boundary is the standard contact 3-sphere $(\mathbb{S}^3, \xi_{\mathrm{st}})$.
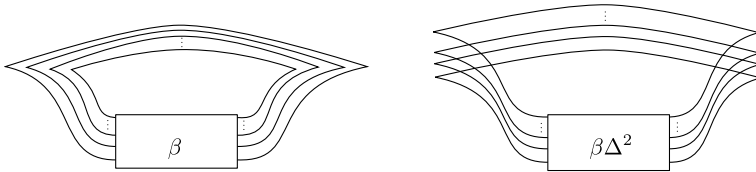
Figure 1. Front projections of the Legendrian isotopic links given as the rainbow closure (left) and (-1)-framed closure (right) of the positive braids β and $\beta\Delta^2$. Here Δ denotes a half twist of the braid.

1.1. Equivalence of Lagrangian fillings

This article has two primary independent contributions, one geometric and the other algebraic. We begin by sketching the two constructions of Lagrangian fillings needed to state our geometric result. The first general method of constructing Lagrangian fillings was given by Ekholm–Honda–Kálmán in [15]. In their construction, a filling L of $\lambda(\beta)$ is given by a series of elementary cobordisms consisting of (1) traces of Legendrian isotopies, (2) pinching cobordisms, which can be seen as 0-resolutions of certain crossings, and (3) minimum cobordisms. In the case of $\lambda(A_{n-1})$, the authors construct a family of L_σ Lagrangian fillings using only pinching and minimum cobordisms, and label them by the permutation σ in S_n specifying an order of resolving the n crossings of $\lambda(A_{n-1})$. The Lagrangian fillings constructed in [15] were then separated into distinct Hamiltonian isotopy classes and indexed to 312-avoiding permutations by Yu Pan in [30], expanding on the Floer-theoretic methods of [15]. The 312-avoiding permutations are permutations σ in S_n avoiding the appearance of numbers ijk, with $i > k > j$, when written in one-line notation. There are a Catalan number $C_n = \frac{1}{n+1}\binom{2n}{n}$ of 312-avoiding permutations in S_n, hence Pan's result shows that there are at least C_n distinct Lagrangian fillings of $\lambda(A_{n-1})$ obtained via pinching cobordisms. These fillings will be referred to as pinching sequence fillings, and the set of (Hamiltonian isotopy classes of) fillings as $\mathcal{P}_n$.

In [37], Treumann and Zaslow gave an alternative construction of a Catalan number of Lagrangian fillings of $\lambda(A_{n-1})$ and distinguished them using the microlocal theory of sheaves. These Lagrangian fillings are represented by planar trivalent graphs and indexed by the triangulated $(n + 2)$-gons dual to such graphs. Given a triangulation $\mathcal{T}$ of a regular $(n + 2)$-gon, we will denote the filling represented by the 2-graph dual to $\mathcal{T}$ by $L_\mathcal{T}$. Casals and Zaslow then generalized the construction of [37] to the setting of positive braid closures in [11] with their construction of Legendrian weaves. We refer to Lagrangian fillings arising from this construction as weave fillings, and denote the set of (Hamiltonian

isotopy classes of) weave fillings of $\lambda(A_{n-1})$ as $\mathcal{W}_n$. We also refer to the elementary cobordism in this construction as a D_4^- cobordism after Arnold's classification of singularities of fronts [1]. In Section 2, we give an explicit description of both a pinching cobordism and a D_4^- cobordism. In Section 3, we produce a Hamiltonian isotopy between the local model describing an elementary pinching cobordism and the local model describing the D_4^- cobordism. This equivalence is then used to prove our first main result:

Theorem 1.1. *For any exact Lagrangian filling of $\lambda(\beta)$ constructed via a sequence of pinching cobordisms and traces of Reidemeister III moves, there is a unique Hamiltonian isotopic weave filling.*

An immediate consequence of Theorem 1.1 is that the two sets of a Catalan number of (Hamiltonian isotopy classes of) exact Lagrangian fillings $\mathcal{W}_n$ and $\mathcal{P}_n$ constructed in [37] and [15] coincide. This confirms statements appearing without proof in [37], Section 2.3, and in [35], Section 6, to that effect. The correspondence is also in agreement with the conjectured ADE-classification of exact Lagrangian fillings (see Conjecture 5.1 in [5]), which predicts precisely C_n distinct fillings of $\lambda(A_{n-1})$ up to Hamiltonian isotopy. Combinatorially, Theorem 1.1 implies that for any 312-avoiding permutation σ, the filling L_σ is Hamiltonian isotopic to the filling $L_\mathcal{T}$ for a unique triangulation $\mathcal{T}$. In Subsection 2.3, we give an explicit recipe for relating σ and the corresponding triangulation $\mathcal{T}_\sigma$ for Hamiltonian isotopic fillings of $\lambda(A_{n-1})$ based on a combinatorial bijection of [33].

1.2. Kálmán loop orbits

Theorem 1.1 appears as a protagonist in another central narrative of our study, an exploration of the orbital structure of the Kálmán loop action on Lagrangian fillings of $\lambda(A_{n-1})$. Introduced by the eponymous mathematician in [26], the Kálmán loop is a Legendrian isotopy that acts on the set of fillings of a Legendrian torus link by permuting the order in which crossings are resolved by elementary cobordism. For weave fillings, the Kálmán loop action is readily understood by the combinatorics of the triangulation of the dual $(n + 2)$-gon under the action of rotation. Theorem 1.1 therefore allows us to geometrically deduce the orbital structure of the Kálmán loop action on the set of pinching sequence fillings where it is otherwise more mysterious.

Second, independently of our geometric result, we also give a Floer-theoretic proof of the orbital structure of the Kálmán loop by examining its action on the augmentation variety $\mathrm{Aug}(\lambda(A_{n-1}))$. The augmentation variety is a Floer-theoretic invariant associated to a Legendrian link. In [15], it was shown that a filling of a Legendrian λ endowed with a choice of a local system can be interpreted geometrically as a point in the augmentation variety $\mathrm{Aug}(\lambda)$. In this way, the augmentation variety can be thought of as a moduli space of fillings for a given Legendrian. The Kálmán loop induces an automorphism of the augmentation variety and we can study this automorphism to understand the orbital structure of the Kálmán loop action on fillings.

In this setting, we introduce our second protagonist, a set of regular functions $\Delta_{i,j}$ on $\mathrm{Aug}(\lambda(A_{n-1}))$, which we show are indexed by diagonals of an $(n + 2)$-gon. These regular functions admit an additional characterization as continuants, recursively defined polynomials studied by Euler in the context of continued fractions [18]. This characterization leads to the appearance of a key supporting character, Euler's identity for continuants.

Continuants naturally appear in the definition of the augmentation variety of $\lambda(A_{n-1})$ (see [8]), and in Section 4 we show that the action of the Kálmán loop is identical to a special case of Euler's identity for continuants. In this sense, we may interpret the Kálmán loop action on the augmentation variety as a Floer-theoretic manifestation of Euler's identity for continuants. Conversely, our geometric story may therefore be characterized as a somewhat convoluted proof of the continuant identity through contact geometry.

Paralleling the geometric story, we prove in Subsection 4.2 that the $\Delta_{i,j}$ give coordinate functions on the toric chart in $\mathrm{Aug}(\lambda(A_{n-1}))$ induced by a pinching sequence filling. From this algebraic argument, we conclude that the orbital structure of the Kálmán loop corresponds precisely to the orbits of triangulations under rotation. The main results of this story are summarized in the two-part theorem below.

Theorem 1.2. *The action of the Kálmán loop on the set $\mathcal{P}_n$, the Catalan number of exact Lagrangian fillings of A-type satisfies*:

(1) *The number of Kálmán loop orbits of fillings of $\lambda(A_{n-1})$ is*

$$\frac{C_n}{n+2} + \frac{C_{n/2}}{2} + \frac{2C_{(n-1)/3}}{3},$$

where the terms with $C_{n/2}$ and $C_{n/3}$ appear if and only if the indices are integers.

(2) *The $\Delta_{i,j}$ functions satisfy the equation*

$$\vartheta(\Delta_{1,k+1}) + (-1)^{n-1}\Delta_{k,n+2} = -\Delta_{2,k}(\Delta_{1,n+2} - 1)$$

as polynomials in $\mathbb{Z}[z_1, \ldots, z_n]$.

Euler's identity for continuants plays a key role in the proof of (2). Following both of our proofs of Theorem 1.2, we conclude our exploration of the Kálmán loop with a discussion of its combinatorial properties. In Subsection 5.1, we describe a method for determining the orbit size of a filling based solely on the associated 312-avoiding permutation.

Theorem 1.3. *There exists an algorithm of complexity $O(n^2)$ with input a 312-avoiding permutation σ in S_n for determining the orbit size of a pinching sequence filling L_σ under the Kálmán loop action.*

In addition, we give an entirely combinatorial description of the Kálmán loop action in terms of 312-avoiding permutations as a sequence of edge flips of triangulations. The appearance of triangulated polygons and edge flips is perhaps best explained as the manifestation of the theory of cluster algebras lurking in the background. While cluster theory does not explicitly appear in any of our proofs, we highlight the connections where relevant. We refer the reader to [7, 10, 23] for more dedicated treatments of cluster structures on the coordinate rings of algebraic varieties associated to Legendrian links.

Remark. As a possible application of Theorem 1.1 beyond Lagrangian fillings of $\lambda(A_{n-1})$, we might hope to describe the orbital structure of fillings of $\lambda(D_n)$ under the action of analogous Legendrian loops. In this context, the combinatorics of tagged triangulations are the D-type analog of the triangulations appearing in A-type. However, there is currently no known combinatorial bijection between tagged triangulations and the D-type Legendrian weaves constructed in [25].

Organization

In Section 2, we cover the necessary preliminaries, including the constructions of exact Lagrangian fillings, the Legendrian contact differential graded algebra, the Kálmán loop, and related combinatorics. Section 3 contains the proof of Theorem 1.1, from which we obtain our geometric proof of Theorem 1.2 as a corollary. In Section 4, we give the Floer-theoretic proof of Theorem 1.2, featuring Euler's identity for continuants. Finally, Section 5 presents the orbit size algorithm of Theorem 1.2, and we conclude with a combinatorial description of the Kálmán loop action on these permutations.

2. Preliminaries on Lagrangian fillings and their invariants

We begin with the necessary preliminaries from contact and symplectic topology. The standard contact structure ξ_{st} in $\mathbb{R}^3$ is the 2-plane field given as the kernel of the 1-form $\alpha = dz - y\,dx$. A link $\lambda \subseteq (\mathbb{R}^3, \xi_{st})$ is Legendrian if λ is always tangent to ξ_{st}. As λ can be assumed to avoid a point, we can equivalently consider Legendrians λ contained in the contact 3-sphere $(\mathbb{S}^3, \xi_{st})$, see [24], Section 3.2.

The symplectization of contact $\mathbb{R}^3$ is the symplectic manifold $(\mathbb{R}_t \times \mathbb{R}^3, d(e^t\alpha))$. Given two Legendrian links λ_- and λ_+, an exact Lagrangian cobordism $L \subseteq (\mathbb{R}_t \times \mathbb{R}^3, d(e^t\alpha))$ from λ_- to λ_+ is a cobordism Σ such that there exists some $T > 0$ satisfying the following:

(1) $d(e^t\alpha)|_\Sigma = 0$,

(2) $\Sigma \cap ((-\infty, T] \times \mathbb{R}^3) = (-\infty, T] \times \lambda_-$,

(3) $\Sigma \cap ([T, \infty) \times \mathbb{R}^3) = [T, \infty) \times \lambda_+$,

(4) $e^t\alpha|_\Sigma = df$ for some function f on Σ.

An exact Lagrangian filling of the Legendrian link $\lambda \subseteq (\mathbb{R}^3, \xi_{st})$ is an exact Lagrangian cobordism L from $\emptyset$ to λ that is embedded in the symplectization $\mathbb{R}_t \times \mathbb{R}^3$. Equivalently, we consider L to be embedded in the symplectic 4-ball with boundary ∂L contained in the contact 3-sphere $(\mathbb{S}^3, \xi_{st})$ (see [2], Section 6.2). For $\lambda(A_{n-1})$, our fillings will be constructed as a series of pinching cobordisms and minimum cobordisms.

We will depict a Legendrian link λ in either of two projections. The front projection $\pi\colon (\mathbb{R}^3, \xi_{st}) \to \mathbb{R}^2$ given by $\pi(x, y, z) = (x, z)$ depicts a projection of λ in the xz-plane. The Lagrangian projection $\Pi\colon (\mathbb{R}^3, \xi_{st}) \to \mathbb{R}^2$ given by $\Pi(x, y, z) = (x, y)$ depicts λ in the xy-plane. In the Lagrangian projection, crossings of $\Pi(\lambda)$ correspond precisely to Reeb chords of λ. Reeb chords are integral curves of the Reeb vector field ∂_z that start and end on λ. In the front projection, the Legendrian condition $T_x\lambda \subseteq \ker(dz - y\,dx)$ implies that $y = dz/dx$. Therefore, Reeb chords are given by pairs of points $(x_1, z_1), (x_2, z_2)$ with $x_1 = x_2$ and $dz_1/dx_1 = dz_2/dx_2$. The key geometric content in Section 3 will involve a careful comparison of Reeb chords in the front and Lagrangian projections of slicings of elementary cobordisms.

2.1. Legendrian weaves

In this subsection we describe Legendrian weaves, the first of two geometric constructions for producing exact Lagrangian fillings of a Legendrian link $\lambda(\beta)$. The key idea of Legendrian weaves is to combinatorially encode a *Legendrian* surface Λ in the 1-jet space $J^1\mathbb{D}^2 = T^*\mathbb{D}^2 \times \mathbb{R}_z$ by the singularities of its front projection in $\mathbb{D}^2 \times \mathbb{R}_z$. The Lagrangian projection of Λ then yields an exact Lagrangian surface in $T^*\mathbb{D}^2$. We describe the general case of Legendrian weave surfaces as given in [11] for the purposes of Theorem 1.1. The case of 2-stranded positive braids is sufficient for all of the content pertaining to Kálmán loop orbits in this paper.

The contact geometric setup of the Legendrian weave construction is as follows. Let β be a positive braid and let

$$\Delta := \prod_{i=1}^{N-1} \prod_{j=1}^{N-i} \sigma_j$$

denote a half twist of the braid. We construct a filling of $\lambda(\beta)$ – equivalently, the (-1)-framed closure of $\beta\Delta^2$, pictured in Figure 1 (right) – by first describing a local model for a Legendrian surface Λ in $J^1\mathbb{D}^2 = T^*\mathbb{D}^2 \times \mathbb{R}_z$. We equip $T^*\mathbb{D}^2$ with the symplectic form $d(e^r\alpha)$ where $\ker(\alpha) = \ker(dy_1 - y_2d\theta)$ is the standard contact structure on $J^1(\partial\mathbb{D}^2)$ and r is the radial coordinate. This choice of symplectic form ensures that the flow of $e^r\alpha$ is transverse to $J^1\mathbb{S}^1 \cong \mathbb{R}^2 \times \partial\mathbb{D}^2$ thought of as the cotangent fibers along the boundary of the 0-section. The Lagrangian projection of Λ is then a Lagrangian surface in $(T^*\mathbb{D}^2, d(e^r\alpha))$. Moreover, since $\Lambda \subseteq (J^1\mathbb{D}^2, \ker(dz - e^r\alpha))$ is a Legendrian, we immediately obtain the function $z : \Pi(\Lambda) \to \mathbb{R}$ satisfying $dz = e^r\alpha|_{\Pi(\Lambda)}$, demonstrating that $\pi(\Lambda)$ is exact.

The boundary of $\Pi(\Lambda)$ is taken to be a positive braid $\beta\Delta^2$ in $J^1\mathbb{S}^1$ so that we regard it as a Legendrian link in a contact neighborhood of $\partial\mathbb{D}^2$. As the 0-section of $J^1\mathbb{S}^1$ is Legendrian isotopic to a max-tb standard Legendrian unknot, we can take $\partial\Pi(\Lambda)$ to equivalently be the standard satellite of the standard Legendrian unknot. Diagramatically, this implies that the braid $\beta\Delta^2$ in $J^1\mathbb{S}^1$ can be given as the (-1)-framed closure of $\beta\Delta^2$ in contact $\mathbb{S}^3$.

2.1.1. N-graphs and singularities of fronts.

To construct a Legendrian weave surface Λ in $J^1\mathbb{D}^2$, we combinatorially encode the singularities of its front projection in a colored graph. Local models for these singularities of fronts are classified by work of Arnold, see Section 3.2 in [1]. The three singularities that appear in our construction describe elementary Legendrian cobordisms and are pictured in Figure 2.

Since the boundary of our singular surface $\pi(\Lambda)$ is the front projection of an N-stranded positive braid, $\pi(\Lambda)$ can be pictured as a collection of N sheets away from its singularities. We describe the behavior at the singularities as follows.

(1) The A_1^2 singularity occurs when two sheets in the front projection intersect. This singularity can be thought of as the trace of a constant Legendrian isotopy in the neighborhood of a crossing in the front projection of the braid $\beta\Delta^2$.

(2) The A_1^3 singularity occurs when a third sheet passes through an A_1^2 singularity. This singularity can be thought of as the trace of a Reidemeister III move in the front projection.
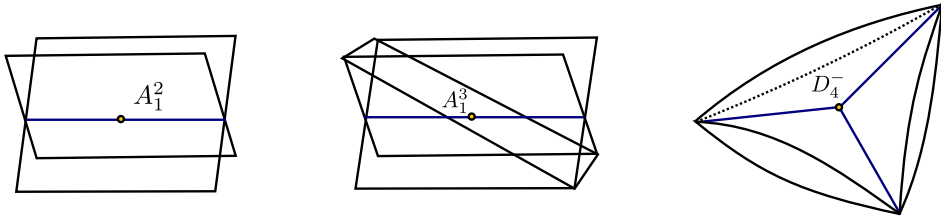
Figure 2. Singularities of front projections of Legendrian surfaces. Labels correspond to notation used by Arnold in his classification.

(3) A D_4^- singularity occurs when three A_1^2 singularities meet at a single point. This singularity can be thought of as the trace of a 1-handle attachment in the front projection.

Having identified the singularities of fronts of a Legendrian weave surface, we encode them by a colored graph $\Gamma \subseteq \mathbb{D}^2$. The edges of the graph are labeled by Artin generators of the braid and we require that any edges labeled σ_i and σ_{i+1} meet at a hexavalent vertex with alternating labels while any edges labeled σ_i meet at a trivalent vertex. To obtain a Legendrian weave $\Lambda(\Gamma) \subseteq (J^1 \mathbb{D}^2, \xi_{st})$ from an N-graph Γ, we glue together the local germs of singularities according to the edges of Γ. First, consider N horizontal sheets $\mathbb{D}^2 \times \{1\} \sqcup \mathbb{D}^2 \times \{2\} \sqcup \cdots \sqcup \mathbb{D}^2 \times \{N\} \subseteq \mathbb{D}^2 \times \mathbb{R}$ and an N-graph $\Gamma \subseteq \mathbb{D}^2 \times \{0\}$. We construct the associated Legendrian weave $\Lambda(\Gamma)$ as follows (see [11], Section 2.3).

- Above each edge labeled σ_i, insert an A_1^2 crossing between the sheets of $\mathbb{D}^2 \times \{i\}$ and $\mathbb{D}^2 \times \{i + 1\}$ so that the projection of the A_1^2 singular locus under $\pi \colon \mathbb{D}^2 \times \mathbb{R} \to \mathbb{D}^2 \times \{0\}$ agrees with the edge labeled σ_i.

- At each trivalent vertex v involving three edges labeled by σ_i, insert a D_4^- singularity between the sheets $\mathbb{D}^2 \times \{i\}$ and $\mathbb{D}^2 \times \{i + 1\}$ in such a way that the projection of the D_4^- singular locus agrees with v and the projection of the A_2^1 crossings agree with the edges incident to v.

- At each hexavalent vertex v involving edges labeled by σ_i and σ_{i+1}, insert an A_1^3 singularity along the three sheets in such a way that the origin of the A_1^3 singular locus agrees with v and the A_1^2 crossings agree with the edges incident to v.

If we take an open cover $\{U_i\}_{i=1}^m$ of $\mathbb{D}^2 \times \{0\}$ by open disks, refined so that any disk contains at most one of these three features, we can glue together the resulting fronts according to the intersection of edges along the boundary of our disks. Specifically, if $U_i \cap U_j$ is nonempty, then we define $\pi(\Lambda(U_1 \cup U_2))$ to be the front resulting from considering the union of fronts $\pi(\Lambda(U_1)) \cup \pi(\Lambda(U_j))$ in $(U_1 \cup U_2) \times \mathbb{R}$.

Definition 2.1. The Legendrian weave $\Lambda(\Gamma)$ contained in $(J^1 \mathbb{D}^2, \xi_{st})$ is the Legendrian surface with front $\pi(\Lambda(\Gamma)) = \pi(\Lambda(\cup_{i=1}^m U_i))$ given by gluing the local fronts of singularities together according to the N-graph Γ.
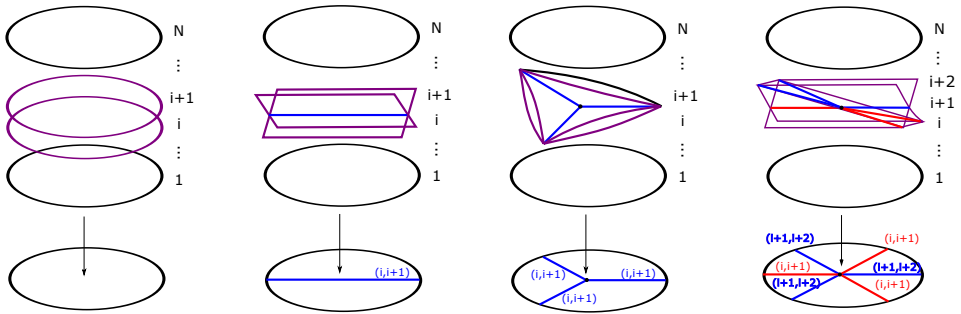
Figure 3. The weaving of singularities of fronts along the edges of the N-graph (courtesy of Roger Casals and Eric Zaslow, used with permission). Gluing these local models according to the N-graph Γ yields the weave $\Lambda(\Gamma)$.

The immersion points of a Lagrangian projection of a weave surface Λ correspond precisely to the Reeb chords of Λ. In particular, if Λ has no Reeb chords, then $\Pi(\Lambda)$ is an embedded exact Lagrangian filling of $\partial(\Lambda)$. In the Legendrian weave construction, Reeb chords correspond to critical points of functions giving the difference of heights between sheets. Every weave surface in this paper admits an embedding where the distance between the sheets in the front projection grows monotonically in the direction of the boundary, ensuring that there are no Reeb chords. See also [37], Subsection 2.3.2.

2.1.2. The D_4^- cobordism. Having described Legendrian weave surfaces, we now define a D_4^- cobordism. As the D_4^- singularity is not a generic Legendrian front singularity, we consider a generic perturbation of the D_4^- singularity, as described in Remark 4.6 of [11] and pictured in Figure 4 (top). A slicing of the Legendrian front, depicted in Figure 4 (bottom), gives a movie of fronts describing the cobordism as follows. Near a Reeb chord trapped between two crossings, we apply a Reidemeister I move and Legendrian isotopy to shrink the Reeb chord. We then add a 1-handle to remove this Reeb chord and apply another pair of Reidemeister I moves to simplify to a diagram with one fewer crossing than we started with. The trace of this movie of fronts forms a surface in $J^1[a,b]$ and yields an exact Lagrangian cobordism in symplectic $\mathbb{R}^4$ by taking the Lagrangian projection of its embedding in contact $\mathbb{R}^5$. By convention, we will identify the remaining crossing with the leftmost crossing of the original pair.

Remark. Note that in our definition of the D_4^- cobordism above, the direction of the arrow in Figure 4 indicates a Lagrangian cobordism from the concave end to the convex end. In contrast, the Legendrian surface given as the Legendrian lift of the (perturbed) D_4^- singularity has no inherent directionality. Nevertheless, in our embedding of the Legendrian weave into $J^1\mathbb{D}^2$, thought of as the contactization of the symplectization of $J^1\mathbb{S}^1$, we choose to orient it so that two of the edges appearing in the D_4^- singularity point towards the boundary in order to project to an embedded exact Lagrangian surface. Indeed, one can see that in cases where we do not require this, our Legendrian weave $\Lambda(\Gamma)$ develops additional Reeb chords that then project to immersed points of $\Pi(\Lambda(\Gamma))$. This subtlety will also be clarified by the fact that the vertical weave construction in the following
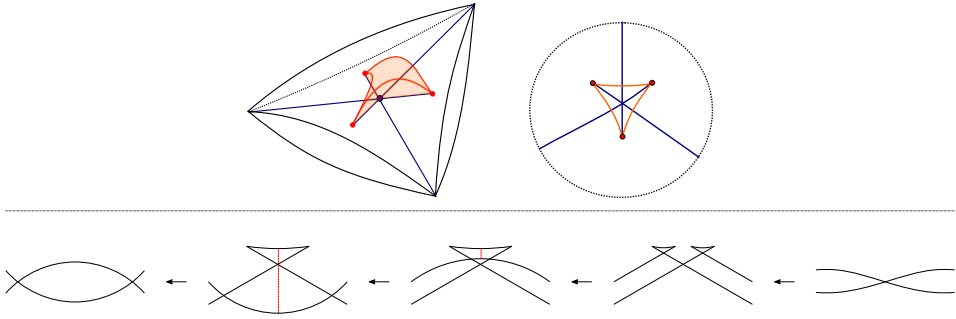
Figure 4. A local model of a generic perturbation of the D_4^- singularity as the front projection of a Legendrian surface (top, courtesy of Roger Casals and Eric Zaslow, used with permission) and as a movie of 1-dimensional fronts (bottom). The Reeb chord is depicted as a dashed red line. We first apply a Reidemeister I move before adding a 1-handle and applying two more Reidemeister I moves to arrive at a diagram with a single crossing.

subsection allows us to unambiguously associate a decomposable exact Lagrangian to a Legendrian weave.

2.1.3. Vertical weaves. In order to relate weave fillings to pinching sequence fillings, we will make use of an equivalent way of describing weaves, combinatorially presented in [8]. This construction arranges the N-graph vertically, with $\partial \mathbb{D}^2$ at the top and the rest of the N-graph appearing below. This construction has the advantage of allowing us to unambiguously associate elementary Lagrangian cobordisms.

Let $\Gamma \subseteq \mathbb{D}^2$ be an N-graph and let $\Lambda(\Gamma) \subseteq J^1(\mathbb{D}^2)$ be the associated weave. In order to produce the associated vertical weave $\Lambda_V(\Gamma)$, we foliate the disk by copies of $\mathbb{S}^1$, as shown in Figure 5 (left). We then consider a diffeomorphism φ taking $\mathbb{D}^2 \backslash \{pt\}$ to $\mathbb{S}^1 \times (-\infty, 0]$. We define φ in such a way that the image of the foliation of $\mathbb{D}^2 \backslash \{pt\}$ is a foliation of $\mathbb{R} \times (-\infty, 0]$ by horizontal lines that are identified at $\pm\infty$ to form a foliation of $\mathbb{S}^1 \times (-\infty, 0]$. The diffeomorphism φ induces a contactomorphism $\tilde{\varphi} : J^1(\mathbb{D}^2) \to J^1(\mathbb{D}^2)$.

Definition 2.2. The vertical weave $\Lambda_V(\Gamma)$ is the Legendrian weave encoded (in the sense of Definition 2.1) by the N-graph $\varphi(\Gamma)$.

After a planar isotopy of Γ, corresponding to a Legendrian isotopy of $\Lambda(\Gamma)$, we can assume that there are no pairs of hexavalent or trivalent vertices appearing in the same horizontal strip $\mathbb{R} \times \{t\}$. The purpose of this modification is to unambiguously decompose a weave filling into elementary Lagrangian cobordisms in order to relate it to a decomposable Lagrangian filling in the symplectization of contact $\mathbb{R}^3$. Other than our manipulation of the ambient contact manifold, the vertical weave construction is identical to the Legendrian weaves described above. See Figure 5 for an example comparing Legendrian weave fillings of $\lambda(A_5)$.

2.1.4. 2-graphs and weave fillings of $\lambda(A_{n-1})$. For our applications involving fillings of $\lambda(A_{n-1})$, we need only consider the case of $N = 2$. Note that 2-graphs are in combinatorial bijection with both binary trees and triangulations of $(n + 2)$-gons, and we will

make use of both of these bijections. In particular, we view the boundary of an $(n + 2)$-gon as a disk so that the 2-graph dual to a triangulation represents a Legendrian weave surface with boundary $\lambda(A_{n-1})$. We list our choice of conventions below for ease of reference.

- In a vertical weave, we encode $\lambda(\beta)$ with the braid word $\Delta\beta\Delta$ appearing at $\mathbb{R} \times \{0\}$.

- In a vertical weave, the edge exiting below a trivalent vertex with incoming edges i and $i + 1$ inherits the label i.

- In a 2-graph Γ dual to a triangulation $\mathcal{T}$, the edge of Γ most immediately clockwise from vertex i of $\mathcal{T}$ is labeled by i.
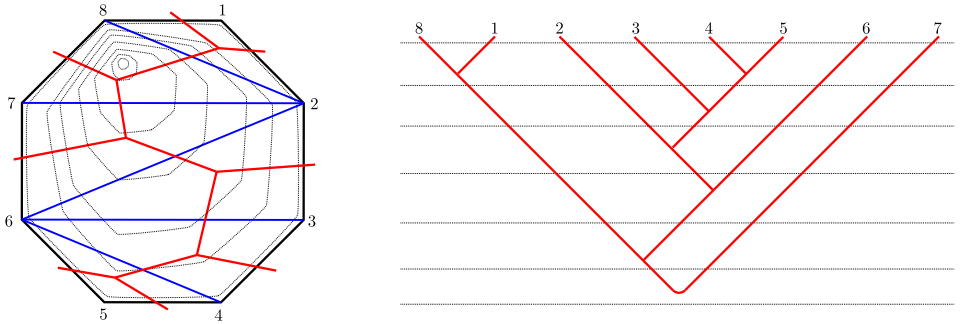
Figure 5. A pair of 2-graphs representing the same weave filling of $\lambda(A_5)$. On the left, the 2-graph Γ is inscribed in its dual triangulation of the octagon. On the right, the corresponding vertical weave is the image of the diffeomorphism φ. The edges of the vertical 2-graph are labeled by the nearest counterclockwise label of the dual triangulation. The dotted lines on the left give a foliation of $\mathbb{D}^2$, corresponding to the foliation of $\mathbb{R} \times (-\infty, 0]$ depicted on the right.

Note that our choice of labeling edges differs slightly from the conventions of [8]. The choice of labeling given there corresponds to resolving the leftmost crossing of the pair in the D_4^- cobordism. With our choice of conventions, we will be able to show that the combinatorial bijection described in Subsection 2.3 relating 312-avoiding permutations to triangulations of the $(n + 2)$-gon yields Hamiltonian isotopic fillings.

2.2. The Legendrian contact DGA and the augmentation variety

In this subsection, we describe the Legendrian contact DGA, a Floer-theoretic invariant of Legendrian knots and their exact Lagrangian fillings. We first give the Ekholm–Honda–Kálmán construction for exact Lagrangian fillings cobordisms, and then describe the necessary Floer-theoretic background.

2.2.1. The pinching cobordism and pinching sequence fillings. The following definition gives a condition for being able to perform a pinching cobordism at a given crossing. See also Definition 6.2 in [15] and Section 2.1 of [9].

Definition 2.3. A crossing in the Lagrangian projection $\Pi(\lambda)$ of a Legendrian λ is contractible if there is a Legendrian isotopy of λ inducing a planar isotopy of $\Pi(\lambda)$ making the length of the corresponding Reeb chord arbitrarily small.

We now describe the precise topological construction of the elementary cobordisms defining pinching sequence fillings. Consider a neighborhood of a contractible crossing depicted in the Lagrangian projection. Attaching a 1-handle at the crossing yields an exact Lagrangian cobordism in the symplectization $(\mathbb{R}_t \times \mathbb{R}^3, d(e^t(dz - y\,dx)))$ (see [15], Section 6.5). In the Lagrangian projection, this 1-handle attachment is diagrammatically given as a 0-resolution of the crossing, as depicted in Figure 6. If λ is the rainbow closure of a positive braid, as is the case for $\lambda(A_{n-1})$, then every crossing of the braid is contractible (see Proposition 2.8 in [9]).
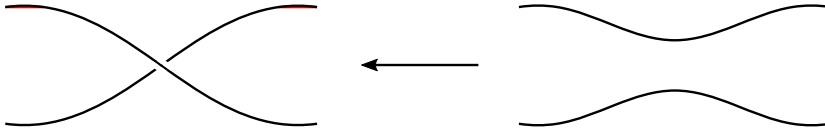
Figure 6. A local model of a pinching cobordism as a 0-resolution of a contractible crossing in the Lagrangian projection. The direction of the arrow indicates a cobordism from the concave end to the convex end.

Let us consider $\lambda \subseteq (\mathbb{R}^3, \xi_{\mathrm{st}})$ and its front projection $\pi(\lambda)$. In order to describe a pinching cobordism in terms of a projection of λ, we introduce the Ng resolution. This is a Legendrian isotopy λ_t such that $\lambda_0 = \lambda$ and the Lagrangian projection $\Pi(\lambda_1)$ can be obtained from the front projection $\pi(\lambda_1)$ by smoothing all left cusps and replacing all right cusps with small loops [29]. See Figure 7 for an example. A pinching cobordism in the front projection of the link $\lambda(\beta)$ is then given by first taking the Ng resolution of $\lambda(\beta)$, performing a 0-resolution at a crossing in the Lagrangian projection as specified above, and then undoing the Ng resolution.
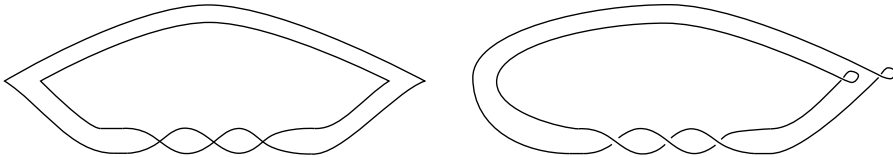
Figure 7. A front projection of $\lambda(A_2)$ (left) and its Ng resolution (right). The three leftmost crossings are contractible.

Given that $\lambda(A_{n-1})$ has n crossings, a pinching sequence filling can be characterized by a permutation σ in S_n. Such a permutation specifies an order in which to apply these elementary cobordisms to the n contractible crossings in the Ng resolution of $\lambda(A_{n-1})$. Given a permutation σ, we will denote it in one line notation $\sigma(1) \ldots \sigma(n)$. If σ is of the form $\sigma(1) \ldots i \, j \ldots k \ldots \sigma(n)$ for $i > k > j$, the permutation $\sigma' = \sigma(1) \ldots j \, i \ldots k \ldots \sigma(n)$ obtained by interchanging i and j gives an order of resolving crossings that yields the same Floer-theoretic invariant[1] [30]. This leads us to consider only a subset of permutations in S_n.

---

[1]The two fillings corresponding to σ and σ' yield identical augmentations ε_σ and $\varepsilon_{\sigma'}$ of the DGA $\mathcal{A}(\lambda(A_{n-1}))$. This is because the presence of the crossing labeled j prevents the existence of any holomorphic

Definition 2.4. A 312-avoiding permutation is a permutation $\sigma \in S_n$ such that any triple of letters i, j, k appearing in order in σ does not satisfy the inequality $i > k > j$.

Distinct 312-avoiding permutations yield distinct Hamiltonian isotopy invariants of exact Lagrangian fillings, i.e., restricting the indexing set from S_n to 312-avoiding permutations yields the existence of at least a Catalan number of fillings of $\lambda(A_{n-1})$ up to Hamiltonian isotopy, see Theorem 1.1 in [30].

2.2.2. The Legendrian contact DGA. For a Legendrian link λ, the Legendrian contact differential graded algebra (DGA) is a powerful Floer-theoretic invariant of λ, see [13]. We denote the DGA of λ by $\mathcal{A}(\lambda; R)$, or by $\mathcal{A}(\lambda)$ when we wish to suppress the dependence on the coefficient ring R. In our description below, we will generally take R to be $\mathbb{Z}[H_1(\lambda)]$ or $\mathbb{Z}[H_1(L)]$ for an exact Lagrangian cobordism L. We refer the interested reader to [17] for a more general introduction to the Legendrian contact DGA, and to [9], Section 3, for a discussion of different choices of coefficient rings.

To describe the algebra $\mathcal{A}(\lambda; R)$, we introduce the auxiliary data of a set of marked points on λ and a corresponding set of capping paths. We label a marked point on the component λ_a of λ by $t_a^{\pm 1}$. In order for the grading to be well defined, we require one marked point for every component of λ and that the oriented tangent vectors to $\Pi(\lambda) \subseteq \mathbb{R}^2_{xy}$ at the marked points $t_1, \ldots, t_m$ are all parallel. Note that the collection $t_1, \ldots, t_m$ of marked points can be thought of as encoding $H_1(\lambda)$. Given a Reeb chord z with ends z_a and z_b lying on components λ_a and λ_b, a capping path γ_z is the concatenation of paths following the orientation of λ from z_a to t_a and t_b to z_b. Here we require that z_a corresponds to the undercrossing of z in the Lagrangian projection. The data of the DGA is then given as follows.

Generators: For a knot λ, the Legendrian contact DGA is freely generated over $R = \mathbb{Z}[t_1^{\pm 1}, \ldots, t_m^{\pm 1}]$ by the Reeb chords of $\lambda \subseteq (\mathbb{R}^3, \xi_{st})$. In the Lagrangian projection, we can equivalently think of these generators as the crossings of λ.

Grading: We restrict our attention to the case of Legendrian links where each component has rotation number zero, as is the case for every link considered in this manuscript. In this setting, each t_i and t_i^{-1} is assigned grading 0. We define the grading for a Reeb chord z as follows. As we traverse the capping path γ_z, the unit tangent vector to $\Pi(\lambda)$ makes a number of counterclockwise revolutions. We can perturb λ in such a way that the tangent vectors at a crossing of $\Pi(\lambda)$ are always orthogonal and the number $r(\gamma_z)$ of such revolutions is always an odd multiple of $1/4$. The grading of z is then defined to be $|z| := 2r(\gamma_z) - 1/2$. Grading is extended to products of generators $|yz|$ additively by $|yz| = |y| + |z|$.

In the case of rainbow closures of a positive braid β, every Reeb chord that corresponds to a crossing of β in the Ng resolution has degree zero while the remaining Reeb chords at the right of the diagram have degree one.

Differential: The differential is given by counts of certain holomorphic disks in the following way. We first decorate each quadrant of a crossing of $\Pi(\lambda)$ with two signs, a

---

strip with positive punctures occurring at both crossings i and k. Therefore, resolving crossing k (respectively, i) has no effect on the generator z_i (respectively, z_k) in the DGA $\mathcal{A}(\lambda(A_{n-1}))$.

Reeb sign and an orientation sign. The Reeb sign is specified as pictured in Figure 8 (left), where opposite quadrants have the same sign and adjacent quadrants have different signs. The orientation sign is given as in Figure 8 (right), where the shaded regions are decorated with orientation sign $-$, and unshaded regions are decorated with orientation sign $+$.
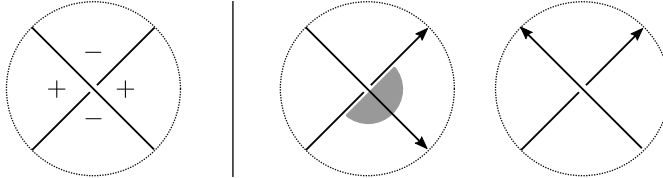
Figure 8. Reeb signs (left) and orientation signs (right) at a crossing of $\Pi(\lambda)$. The quadrants shaded dark gray carry negative orientation signs, while the unshaded quadrants are positive.

The differential considers immersions u from a punctured disk into $\mathbb{R}^2$ with boundary punctures on $\Pi(\lambda)$ up to reparametrization. We refer to any puncture appearing at a quadrant with a positive (respectively, negative) Reeb sign as a positive (respectively, negative) puncture. We restrict to immersions that have a single positive puncture and arbitrarily many negative punctures. For any such immersion u, denote by $w(u)$ the product of generators given by the negative boundary punctures. If the boundary of u passes through any marked point t_i, then we obtain $w'(u)$ as the product of $w(u)$ by $t_i^{\pm 1}$. The power is assigned according to whether the orientation of u at the relevant marked point agrees (t_i) with the orientation of λ or does not agree (t_i^{-1}) with the orientation of λ. To each disk u, we also assign the quantity $\mathrm{sgn}(u) \in \{\pm 1\}$ given by the product of the orientation signs appearing at boundary punctures of u. The differential at z is then given by

$$\partial(z) = \sum \mathrm{sgn}(u)\, w'(u)$$

where the sum is taken over all immersed disks u with a single positive puncture at z. We extend the differential to products $z_1 z_2$ by the Leibniz rule

$$\partial(z_1 z_2) = \partial(z_1)\, z_2 + (-1)^{|z_1|}\, z_1\, \partial(z_2).$$

Example. The DGA of $\lambda(A_2)$ is freely commutatively generated over $\mathbb{Z}[t, t^{-1}]$ by generators a_1, a_2, z_1, z_2, z_3, labeled in Figure 9. The gradings are given by $|a_1| = |a_2| = 1$ and $|z_i| = |t_1| = 0$. The differential on generators a_i is given by

$$\partial(a_i) = \begin{cases} z_1 + z_3 + z_1 z_2 z_3 + t_1^{-1} & \text{for } i = 1, \\ 1 + t_1 + z_2 + t_1 z_3 z_2 + t_1 z_1 z_2 + t_1 z_1 z_2 z_3 z_2 & \text{for } i = 2. \end{cases}$$

The differential on the remaining generators vanishes for degree reasons. Note that setting $t_1 = -1$ implies $\partial(a_2) = -z_2 \partial(a_1)$

2.2.3. Augmentations. The Legendrian contact DGA can be difficult to extract information from, so it is often useful to consider augmentations of the DGA. Augmentations are
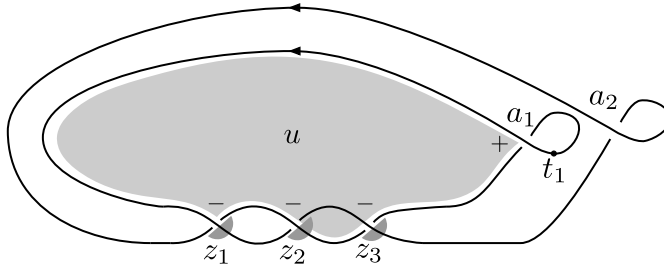
Figure 9. The Lagrangian projection of the Legendrian trefoil decorated with Reeb signs and orientation signs. The light gray disk labeled u has a positive puncture at a_1 and a single negative puncture at z_1. Thus, it corresponds to the term z_1 appearing in $\partial(a_1)$.

DGA maps from $\mathcal{A}(\lambda)$ to some ground ring. Here we consider the ground ring of Laurent polynomials in $n - 1$ variables with coefficients in $\mathbb{Z}$, understood as a DGA with trivial differential and concentrated in degree 0. In this subsection, we define augmentations and the related Legendrian isotopy invariant, the augmentation variety.

Augmentations of $\mathcal{A}(\lambda)$ are intimately tied to Lagrangian fillings of λ. This relationship can be understood through the functoriality of the DGA with respect to exact Lagrangian cobordisms. More precisely, Ekholm–Honda–Kálmán show (Theorem 1.2 in [15]) that an exact Lagrangian cobordism L from λ_- to λ_+ induces a DGA map Φ_L from $\mathcal{A}(\lambda_+; \mathbb{Z}_2)$ to $\mathcal{A}(\lambda_-; \mathbb{Z}_2)$. Their result was upgraded to make use of $\mathbb{Z}_2[H_1(L)]$ coefficients with an appropriate choice of marked points encoding $H_1(L)$ by Pan (Proposition 2.6 in [30]). Pan's use of $H_1(L)$ coefficients is crucial for her ability to distinguish C_n Lagrangian fillings of $\lambda(A_{n-1})$, as Ekholm–Honda–Kálmán are only able to identify $(2^{n+1} - (-1)^{n+1})/3$ distinct Lagrangian fillings working over $\mathbb{Z}_2$ (Theorem 1.6 in [15]). The following result of Karlsson further improves Pan's coefficient ring to consider the augmentations over $\mathbb{Z}[H_1(L)]$.

Proposition 2.5 (Theorem 2.5 in [28]). *An exact Lagrangian cobordism L from λ_- to λ_+ induces a DGA map $\Phi_L \colon \mathcal{A}(\lambda_+; \mathbb{Z}[H_1(\lambda_+)]) \to \mathcal{A}(\lambda_-; \mathbb{Z}[H_1(L)])$.*

See also Section 3.3 of [9] for a discussion on Karlsson's choice of signs, as well as a geometric understanding of the induced map. As a result of Proposition 2.5, we can think of an augmentation of λ as a map induced from $\mathcal{A}(\lambda; \mathbb{Z}[H_1(\lambda)])$ to the DGA of the empty set induced by an exact Lagrangian filling of λ.

Definition 2.6. An augmentation ε_L induced by a Lagrangian filling L of λ is a DGA map

$$\varepsilon_L : \mathcal{A}(\lambda, \mathbb{Z}[H_1(\lambda)]) \to \mathbb{Z}[H_1(L)],$$

where we think of $\mathbb{Z}[H_1(L)]$ as a DGA concentrated in degree zero with trivial differential.

The functoriality of the DGA motivates the study of augmentations of $\mathcal{A}(\lambda)$ in order to better understand Lagrangian fillings of λ. The space of all augmentations of $\mathcal{A}(\lambda)$, denoted by $\mathrm{Aug}(\lambda)$, is an invariant of λ. In the case where λ is the rainbow closure of

a positive braid, $\mathrm{Aug}(\lambda)$ has the structure of an affine algebraic variety and is known as the augmentation variety. We tensor our coefficients ring with $\mathbb{C}$ in order to consider augmentations over a field.[2] When the grading of $\mathcal{A}(\lambda)$ is concentrated in non-negative degrees, as is the case for rainbow closures of positive braids, then $\mathrm{Aug}(\lambda) \cong \mathrm{Spec}\, H_0(\mathcal{A}(\lambda))$, see e.g. Corollary 2.9 in [23]. Since Spec is contravariant, ε_L induces a map $\mathrm{Spec}(\mathbb{C}[s_1^{\pm 1}, \ldots, s_{b_1(L)}^{\pm 1}]) \to \mathrm{Spec}\, H_0(\mathcal{A}(\lambda; \mathbb{C}[H_1(\lambda)]))$, where we have identified the ground ring of Laurent polynomials with complex coefficients $\mathbb{C}[H_1(L)]$ with the group ring $\mathbb{C}[s_1^{\pm 1}, \ldots, s_{b_1(L)}^{\pm 1}]$. We interpret this map as the inclusion of a toric chart $(\mathbb{C}^\times)^{b_1(L)}$ into the augmentation variety

$$\mathrm{Spec}(\mathbb{C}[s_1^{\pm 1}, \ldots, s_{b_1(L)}^{\pm 1}]) \cong (\mathbb{C}^\times)^{b_1(L)} \hookrightarrow \mathrm{Aug}(\lambda).$$

The image of degree-zero generators under an augmentation give local coordinate functions on the corresponding toric chart. In order to describe these local coordinate functions, we discuss Pan's explicit computation of induced DGA maps in the context of Lagrangian fillings of $\lambda(A_{n-1})$ with a lift to $\mathbb{Z}[H_1(L)]$ following [9], Section 4.2. For a pinching cobordism, the induced map is given by a certain count of holomorphic disks, similar to the differential. The homology coefficients are determined by the intersection of these disks with relative homology classes in $H_1(L, \lambda_- \sqcup \lambda_+)$, which is identified with $H_1(L)$ via Poincaré duality.

Pan describes a set of generators for $H_1(L, \lambda_- \sqcup \lambda_+)$ for a sequence of pinching cobordisms. In this setting, a relative homology cycle $\gamma_{\sigma(i)}$ starts from the saddle point originally labeled $z_{\sigma(i)}$ and extends downwards to λ_- where it meets the boundary in $s_{\sigma(i)}$ and $s_{\sigma(i)}^{-1}$. In order to consider signs, we orient this relative cycle so that the two halves of the cycle are labeled by $s_{\sigma(i)}$ and $-s_{\sigma(i)}^{-1}$, as in Figure 10. In a slicing of the symplectization, $\gamma_{\sigma(i)}$ meets the Lagrangian projection of $\lambda(A_k)$ in two points labeled $s_{\sigma(i)}$ and $-s_{\sigma(i)}^{-1}$, so that in practice, these generators reduce the computation of the coefficients to a combinatorial count of marked points.

Given a pinching cobordism $L_{\sigma(i)}$ at the Reeb chord $z_{\sigma(i)}$ as part of a Lagrangian filling L_σ, the induced map Φ_i on the generator z_j is computed as a sum over all immersed disks with positive punctures at both $z_{\sigma(i)}$ and z_j. As before, we denote by $w'(u)$ the product of negative punctures of the immersed disk u and intersections of u with marked points counted with orientation. Likewise, $\mathrm{sgn}(u)$ is given by the product of the orientation signs appearing at boundary punctures of u.

**Definition 2.7.** The DGA map Φ_i induced by a pinching cobordism at the Reeb chord $z_{\sigma(i)}$ is given by

$$\Phi_i(z_j) = z_j + \sum \mathrm{sgn}(u)\, w'(u).$$

The Reeb chord $z_{\sigma(i)}$ is sent to $s_{\sigma(i)}$ by Φ_i.
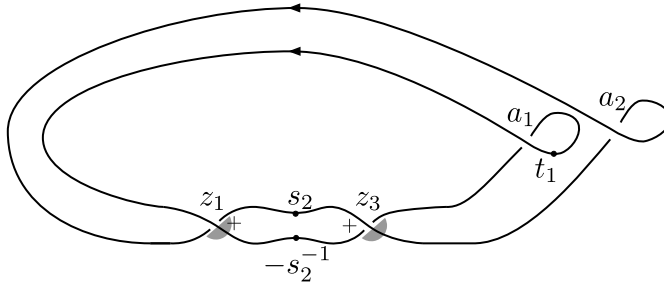
Example. Pinching at the Reeb chord labeled by z_2 of the Legendrian trefoil pictured in Figure 9 yields the Legendrian Hopf link, pictured in Figure 11 with the addition of

---

[2]To clarify, complexifying is solely for the purpose of simplifying the algebro-geometric discussion in this paragraph. For all other purposes, we will continue to use integer coefficients.
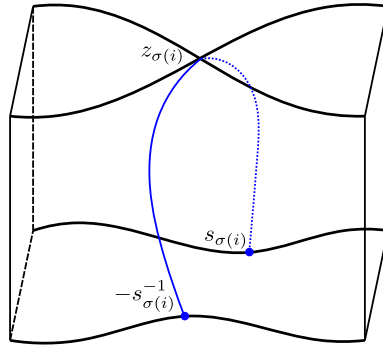
Figure 10. A local model of a relative cycle encoding the homology of a pinching cobordism L. At the top of the figure, the length of the Reeb chord $z_{\sigma(i)}$ is 0, i.e., the two strands intersect at the point $z_{\sigma(i)}$. The bottom of the figure depicts a 0-resolution of the crossing where marked points labeled $-s_{\sigma(i)}^{-1}$ and $s_{\sigma(i)}$ encode $H_1(L)$.

Figure 11. A Legendrian Hopf link obtained from the knot pictured in Figure 9 by pinching at the Reeb chord labeled by z_2.

marked points s_2 and $-s_2^{-1}$. The induced map Φ_1 on the DGA is given by

$$z_1 \mapsto z_1 - s_2^{-1}, \quad z_2 \mapsto s_2, \quad z_3 \mapsto z_3 - s_2^{-1}.$$

Performing another pinch at z_1 induces the map Φ_2 given by

$$z_1 \mapsto s_1, \quad s_2 \mapsto s_2, \quad z_3 \mapsto z_3 + s_1^{-1}s_2^{-2}.$$

The map on z_3 is determined by the disk with positive punctures at z_1 and z_3 passing through s_2 and $-s_2^{-1}$.

Pan gives a purely combinatorial description of the map Φ_i induced by opening the crossing labeled $z_{\sigma(i)}$ (see Definition 3.2 in [30]). First, define the set

$$T_\sigma^i = \{j \in \{1, \ldots, n\} \mid \sigma^{-1}(j) > \sigma^{-1}(i) \text{ and if } i < k < j \text{ or } j < k < i,$$
$$\text{then } \sigma^{-1}(k) < \sigma^{-1}(i)\}.$$

For $j \in T_\sigma^{\sigma(i)}$ and $1 \leq i \leq n$, the DGA map with coefficients in $\mathbb{Z}_2[H_1(L)]$ is given by

$$\Phi_i(z_j) = z_j + s_{\sigma(i)}^{-1} \prod_{\substack{j < k < \sigma(i) \text{ or} \\ \sigma(i) < k < j}} s_k^{-2},$$

and for $j = \sigma(i)$, $\Phi_i(z_j) = s_j$. Otherwise, we take Φ_i to be the identity.

Lemma 2.8. *The lift of Pan's combinatorial formula for Φ_i to $\mathbb{Z}[H_1(L)]$ is given by*

$$\Phi_i(z_j) = z_j + (-1)^{|j-\sigma(i)|+1} s_{\sigma(i)}^{-1} \prod_{\substack{j < k < \sigma(i) \text{ or} \\ \sigma(i) < k < j}} s_k^{-2}.$$

Proof. To upgrade Pan's formula to $\mathbb{Z}[H_1(L)]$ coefficients, we note that the number of pairs of marked points that appear between z_j and $z_{\sigma(i)}$ is precisely $|j - \sigma(i)|$. Since each pair of marked points contributes a -1 factor to $\text{sgn}(u)$ and the disk u with positive punctures at z_j and $z_{\sigma(i)}$ picks up an additional -1 factor from the orientation sign of the leftmost positive puncture, we arrive at the formula given above. ∎

To compute an augmentation of $\mathcal{A}(\lambda; \mathbb{Z}[T])$, we also need to describe the map induced by the minimum cobordism. This minimum cobordism is given by filling a standard Legendrian unknot λ_U with an exact Lagrangian disk. It induces a map $\Phi_{\min}$ sending the Reeb-chord generator of $\mathcal{A}(\lambda_U; \mathbb{Z}[T])$ to 0. The map on the marked point generators can be deduced from the fact that $\Phi_{\min}$ is a DGA map and therefore we must have $\Phi_{\min} \circ \partial = 0$. In the context of a filling L_σ of $\lambda(A_{n-1})$, this tells us that $s_1 \ldots s_n + t_1 = 0$. For knots, we also obtain $-(s_1 \ldots s_n)^{-1} + 1 = 0$, implying that t_1 is mapped to -1. For links, we have $(s_1 \ldots s_n)^{-1} + t_2 = 0$, implying only that $t_1 t_2 = 1$. Pan avoids this ambiguity by computing augmentations of $\mathcal{A}(\lambda(A_{2n-1}; H_1(\lambda(A_{2n-1}))$ induced by fillings L_σ of $\lambda(A_n)$ where $\sigma(1) = n + 1$. This is equivalent to setting $t_1 = -1$, from which we obtain $t_2 = -1$. Therefore, the DGA map induced by the minimum cobordism is given by the following formula:

$$\Phi_{\min}(s_n) = s_1^{-1} \ldots s_{n-1}^{-1}.$$

For $s_i \neq s_n$, $\Phi_{\min}$ is the identity map. For marked points t_i, we have $\Phi_{\min}(t_i) = -1$.

Together, the maps Φ_i and $\Phi_{\min}$ give us the ingredients to define the augmentation induced by a pinching sequence filling of $\lambda(A_{n-1})$.

Definition 2.9. The augmentation ε_{L_σ} induced by the Lagrangian filling L_σ of $\lambda(A_{n-1})$ is given by the DGA map $\varepsilon_{L_\sigma} := \Phi_{\min} \circ \Phi_n \circ \cdots \circ \Phi_1$.

To simplify our computations involving the DGA and the Kálmán loop, we will always set $t_1 = -1$ and $t_2 = -1$ for the remainder of this manuscript. By our definition of ε_{L_σ}, this does not affect the augmentation induced by L_σ.

2.2.4. Braid matrices. For $\lambda(A_{n-1})$, the polynomials defining the augmentation variety have a combinatorial description as a specific entry in a product of matrices. These matrices originally appeared in [27] as a means for encoding the immersed disks contributing to the differential. More recently, they were used in [8] to give a holomorphic symplectic structure on the augmentation variety. We adopt the conventions of [8] in defining the braid matrix.

Definition 2.10. The braid matrix $B(z_i)$ is given by

$$B(z_i) := \begin{pmatrix} 0 & 1 \\ 1 & z_i \end{pmatrix}.$$

Intuitively, one can think of the matrix $B(z_i)$ as encoding whether or not an immersed disk has a negative puncture at the crossing labeled by z_i. A product of braid matrices can be used to compute the differential of $\mathcal{A}(\lambda(A_{n-1}); \mathbb{Z})$ as follows. First, label the crossings of $\lambda(A_{n-1})$ by $a_1, a_2, z_1, \ldots, z_n$, as in Figure 9. From Section 3.1 in [27], we have that $\partial(a_1) = -1 + \left[\prod_{i=1}^{n} B(z_i)\right]_{(2,2)}$ where the subscript denotes the $(2, 2)$ entry of the product, and the -1 appears due to our choice of conventions. See also Proposition 5.2 in [9] for a similar computation. An analogous computation to the case of $\lambda(A_2)$ implies that the differential of a_2 is given by $\partial(a_2) = -\Delta_{2,n+1}(\partial(a_1))$.

The computation of the differential via braid matrices also allows us to express the augmentation variety $\text{Aug}(\lambda(A_{n-1}))$ in a similar manner. As augmentations are DGA maps, they satisfy $\varepsilon \circ \partial = \partial \circ \varepsilon$. Since ε respects the grading, it must vanish on generators of nonzero degree, implying that for such generators a, we have $\partial \circ \varepsilon(a) = 0$. Therefore, any augmentation ε of $\mathcal{A}(\lambda(A_{n-1}))$ satisfies $\varepsilon \circ \partial(a_1) = \partial(a_2) = 0$. Since $\partial(a_2)$ is a multiple of $\partial(a_1)$, the vanishing of $\partial(a_1)$ is both necessary and sufficient to satisfy the vanishing condition for $\varepsilon \circ \partial$, so that the augmentation variety is cut out by the vanishing of the equation $\partial(a_1) = 0$.

Lemma 2.11. *The augmentation variety* $\text{Aug}(\lambda(A_{n-1}))$ *is the zero set of the polynomial*

$$X_n := -1 + \left[\prod_{i=1}^{n} B(z_i)\right]_{(2,2)}.$$

In addition to computing the augmentation variety, braid matrices also define regular functions $\Delta_{i,j}$ on $\text{Aug}(\lambda(A_{n-1}))$ that will play an important role in Section 4.

Definition 2.12. The regular function $\Delta_{i,j} \in \mathbb{Z}[X_n]$ is given by

$$\Delta_{i,j} := \left[\prod_{k=i}^{j-2} B(z_k)\right]_{(2,2)}.$$

We specify the value of $\Delta_{i,i+1}$ to be 1. We collect some useful identities relating the $\Delta_{i,j}$ functions to the theory of continuants below.

Example. Consider the Legendrian trefoil, $\lambda(A_2)$. The augmentation variety $\text{Aug}(\lambda(A_2))$ is the zero set of the polynomial $X_3 = -1 + z_1 + z_3 + z_1 z_2 z_3$. The regular functions $\Delta_{i,j}$ are of the form $\Delta_{i,i+2} = z_i$ or $\Delta_{i,i+3} = 1 + z_i z_{i+1}$, for $1 \leq i \leq 3$.

2.2.5. Continuants. Continuants are a family of polynomials $K_n(x_1, \ldots, x_n)$ studied by Euler in his work on continued fractions [18]. Continuants are defined by the following recursive formula:

$$K_n(x_1, \ldots, x_n) = x_1 K_{n-1}(x_2, \ldots, x_n) + K_{n-2}(x_3, \ldots, x_n),$$
$$K_0() = 1, \quad K_1(x_1) = x_1.$$

As mentioned above, the regular functions $\Delta_{i,j}$ are related to continuants.

Lemma 2.13. *Let $n = j - 2 - i$ and $x_k = z_{i+k-1}$. Then*

$$K_n(x_1, \ldots, x_n) = \Delta_{i,j}.$$

Proof. The following is a classical property of continuants (see e.g. [22], Section 1) that allows us to understand the defining recursion relation in terms of braid matrices:

$$\begin{pmatrix} K_{n-2}(x_2, \ldots, x_{n-1}) & K_{n-1}(x_2, \ldots, x_n) \\ K_{n-1}(x_1, \ldots, x_{n-1}) & K_n(x_1, \ldots, x_n) \end{pmatrix} = B(x_1) \cdots B(x_n).$$

This follows inductively from applying the recursion relation in computing the matrix product:

$$\begin{pmatrix} 0 & 1 \\ 1 & x_1 \end{pmatrix} \begin{pmatrix} K_{n-3}(x_3, \ldots, x_{n-1}) & K_{n-2}(x_3, \ldots, x_n) \\ K_{n-2}(x_2, \ldots, x_{n-1}) & K_{n-1}(x_2, \ldots, x_n) \end{pmatrix}$$
$$= \begin{pmatrix} K_{n-2}(x_2, \ldots, x_{n-1}) & K_{n-1}(x_2, \ldots, x_n) \\ K_{n-1}(x_1, \ldots, x_{n-1}) & K_n(x_1, \ldots, x_n) \end{pmatrix}.$$

Therefore,

$$K_n(x_1, \ldots, x_n) = \Big[\prod_{k=1}^n B(x_k) \Big]_{(2,2)}.$$

Replacing x_k with z_{i+k-1} yields the desired identification. ∎

As a consequence, we obtain the following continuant recursion relation in the context of the $\Delta_{i,j}$ functions:

$$(2.1) \qquad \Delta_{i,j} = z_i \, \Delta_{i+1,j} + \Delta_{i+2,j}$$

Continuants satisfy several identities, the most general of which is Euler's identity for continuants. We present this identity in the context of the $\Delta_{i,j}$ functions:

$$\Delta_{1,\mu+\nu+2} \, \Delta_{\mu+1,\mu+\kappa+2} - \Delta_{1,\mu+\kappa+2} \, \Delta_{\mu+1,\mu+\nu+2} = (-1)^{\kappa+1} \, \Delta_{1,\mu+1} \, \Delta_{\mu+\kappa+2,\mu+\nu+2}$$

for $\mu \geq 1, \kappa \geq 0, \nu \geq \kappa + 1$ [38]. We require a special case of this identity for our algebraic proof of Theorem 1.2. Namely, when $\mu = 1, \kappa = k - 3 \geq 0, \nu = n - 1 \geq k - 2$, we obtain

$$(2.2) \qquad \Delta_{1,n+2} \, \Delta_{2,k} - \Delta_{1,k} \, \Delta_{2,n+2} = (-1)^k \, \Delta_{1,2} \, \Delta_{k,n+2}.$$

2.2.6. The Kálmán loop. In [26], Kálmán defined a geometric operation on Legendrian torus links that induces an action on their exact Lagrangian fillings. In the case of $\lambda(A_{n-1})$, this operation consists of a Legendrian isotopy that is visualized by dragging the leftmost crossing clockwise around the link until it becomes the rightmost crossing. The graph of this isotopy is an exact Lagrangian cylinder in the symplectization of $(\mathbb{R}^3, \xi_{\mathrm{st}})$. Concatenating this cylinder with a Lagrangian filling L of $\lambda(A_{n-1})$ yields another filling, generally not Hamiltonian isotopic to L. As computed in Proposition 9.1 of [26], this induces a map on the DGA $\mathcal{A}(\lambda(A_{n-1}); \mathbb{Z}_2)$, which in turn induces an automorphism ϑ on the augmentation variety $\mathrm{Aug}(\lambda(A_{n-1}))$. Following Section 3 of [9], we can compute this induced action with integer coefficients. The additional information of this integral lift

consists solely of a choice of signs for terms in the image of ϑ, as can be seen in Kálmán's example computation over $\mathbb{Z}[t, t^{-1}]$ in the case of the $\lambda(A_2)$ (see Section 5 in [26]).[3] The map ϑ on generators z_i is then given by

$$\vartheta(z_i) = \begin{cases} -\Delta_{2,n+2} & \text{for } i = 1, \\ z_{i-1} & \text{for } 2 \leq i \leq n. \end{cases}$$

For the $\Delta_{i,j}$ functions, this is expressed as $\vartheta(\Delta_{i,j}) = \Delta_{i-1,j-1}$ for $i > 1$, and

$$\vartheta(\Delta_{1,j}) = -\left[B(\Delta_{2,n+2}) \prod_{i=1}^{j-3} B(z_i) \right]_{(2,2)}.$$

2.3. Combinatorics of triangulations

The two geometric constructions of Lagrangian fillings discussed above, as well as their algebraic invariants involve combinatorial characterizations that are crucial for our later description of the action of the Kálmán loop. This subsection starts with a description of the specific combinatorial bijection between 312-avoiding permutations σ and triangulations $\mathcal{T}_\sigma$ that we use to relate the Lagrangian fillings L_σ and $L_{\mathcal{T}_\sigma}$. We then describe the orbital structure of triangulations under the action of rotation, and conclude with a combinatorial description of the set of triangulations in terms of the flip graph.

2.3.1. The clip sequence bijection. As a first step towards relating pinching sequence fillings and weave fillings, we describe a combinatorial bijection between triangulations of the $(n + 2)$-gon and 312-avoiding permutations in S_n. As a corollary to Theorem 1.1, we will show that this combinatorial bijection corresponds to a Hamiltonian isotopy of the Lagrangian fillings defined by this input data.

For a 312-avoiding permutation σ, we denote the corresponding triangulation by $\mathcal{T}_\sigma$ and a diagonal between vertex i and vertex j of $\mathcal{T}_\sigma$ by $D_{i,j}$. Adopting the terminology of [33], we refer to a triangle in $\mathcal{T}_\sigma$ with sides $D_{i,i+2}, D_{i,i+1}, D_{i+1,i+2}$, two of which lie on the $(n + 2)$-gon, as an ear of the triangulation. Note that any triangulation must have at least two ears and that the middle vertex of an ear necessarily has no diagonal incident to it.

Given a triangulation of the $(n + 2)$-gon, the clip sequence bijection is defined as follows. First, label the vertices in clockwise order from 1 to $n + 2$. Remove the middle vertex of the ear with the smallest label, record the label and delete all edges of the $(n + 2)$-gon incident to the vertex. Repeat this process with the ear whose middle vertex is now the smallest of the remaining vertices in the resulting triangulation of the $(n + 1)$-gon. Continue this process until no triangles remain. The main result of [33] is that this map is indeed a bijection between the set of 312-avoiding permutations in S_n and triangulations of the $(n + 2)$-gon.

The clip sequence bijection allows us to explicitly define a weave filling with the input of a 312-avoiding permutation σ.

---

[3]Note that Kálmán uses a different choice of sign conventions than Casals and Ng. By Proposition 3.14 in [9], these different sign conventions yield equivalent induced augmentations.

Definition 2.14. The Lagrangian filling $L_{\mathcal{T}_\sigma}$ is the weave filling defined by the 2-graph dual to the triangulation $\mathcal{T}_\sigma$.

See Figure 12 for a computation of the 312-avoiding permutation corresponding to the triangulation dual to the 2-graph example given above.
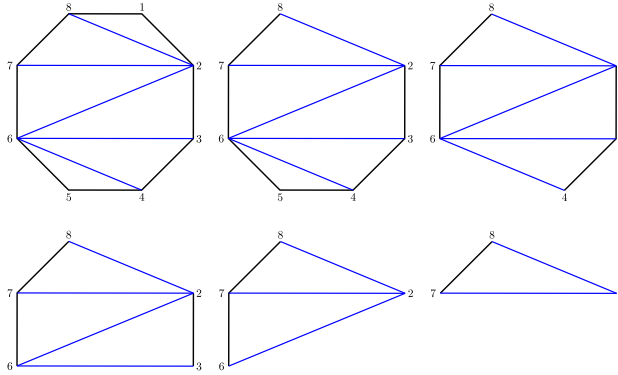
Figure 12. An example computation of the clip sequence bijection. Starting with our initial triangulation, we remove and record the smallest numbered vertex with no incident diagonals. From the sequence pictured, we get the 312-avoiding permutation $\sigma = 154362$. The diagonal $D_{2,8}$ yields the function $\Delta_{1,3}$ after adding 1 to both indices and reducing mod 8.

2.3.2. Orbits of triangulations under rotation. In Section 4, we shall show that, in $\mathrm{Aug}(\lambda)$, the global functions $\Delta_{i,j}$ transform as $\vartheta(\Delta_{i,j}) = \Delta_{i-1,j-1}$ for indices taken modulo $n + 2$. As suggested by our weave fillings, we can also consider the $\mathbb{Z}_{n+2}$ action of counterclockwise rotation on the set of diagonals $\{D_{i,j}\}_{\mathcal{T}}$ of a triangulation $\mathcal{T}$ of the $(n + 2)$-gon. Restricting to the toric chart induced by an augmentation σ, there is a corresponding triangulation $\mathcal{T}_\sigma$ for which it can be shown that the set map $D_{i-1,j-1} \mapsto \Delta_{i,j}$ between diagonals $\{D_{i-1,j-1}\}_{\mathcal{T}_\sigma}$ of the triangulation $\mathcal{T}_\sigma$ and regular functions $\{\Delta_{i,j}\}$ is a $\mathbb{Z}_{n+2}$-equivariant map.[4] The orbital structure of the action of rotation on triangulations will therefore appear as a crucial ingredient in the proofs of Theorems 1.2.

The number of orbits of the set of triangulations of the $(n + 2)$-gon under the action of counterclockwise rotation is given by the formula

$$\frac{C_n}{n + 2} + \frac{C_{n/2}}{2} + \frac{2\,C_{(n-1)/3}}{3},$$

where, as previously, the terms with $C_{n/2}$ and $C_{n/3}$ only appear if the indices are integers. These terms correspond, respectively, to triangulations with no rotational symmetry, rotational symmetry by π, and rotational symmetry by $2\pi/3$. No other rotational symmetry of a triangulation is possible. The orbit sizes are $n + 2$, $(n + 2)/2$ and $(n + 2)/3$, where again the corresponding orbit size only occurs if the relevant fraction is an integer.

---

[4]As we explain later, this indexing shift is necessary so that the combinatorial bijection between 312-avoiding permutations and triangulations yields Lagrangian fillings that induce the same toric chart inside the augmentation variety.

2.3.3. The flip graph. The combinatorics of triangulations of the $(n + 2)$-gon have previously appeared in constructions of A-type fillings. As explained in [11, 37], Legendrian mutation, an operation for generating new fillings, corresponds to exchanging diagonals of a quadrilateral in the original triangulation to form a new triangulation. Such an exchange of diagonals is depicted in Figure 18, and we refer to it as an edge flip. See Subsection 4.3 for more on the cluster-algebraic interpretation of this operation in terms of cluster mutation. The flip graph or associahedron is then defined to have vertices given by triangulations and an edge between two vertices if the triangulations are related by a single edge flip. The diameter of the flip graph was first investigated via geometric methods by Thurston, Sleator and Tarjan in [34] and later combinatorially by Pournin in [32]. In general, the combinatorics of the flip graph are an area of active interest, and there is no known algorithm for determining geodesics. In Subsections 5.2 and 5.3, we present a description of the Kálmán loop as a sequence of edge flips in the flip graph and describe the result of a single edge flip on a 312-avoiding permutation, thus providing a characterization of the Kálmán loop action as a geodesic path in the flip graph.

3. Isotopies of exact Lagrangian cobordisms

In this section we prove that a pinching sequence filling L_σ is Hamiltonian isotopic to the weave filling $L_{\mathcal{T}_\sigma}$ for a given 312-avoiding permutation σ. We first relate the elementary cobordisms used to construct these fillings.

Proposition 3.1. *The pinching cobordism and D_4^- cobordism are Hamiltonian isotopic relative to their boundaries.*

We prove this by giving a local model for the D_4^- cobordism as a sequence of diagrams in both the front and Lagrangian projections and then describing an exact Lagrangian isotopy between the two cobordisms that fixes the boundary. Since compactly supported Lagrangian isotopy is equivalent to Hamiltonian isotopy (see Theorem 3.6.7 in [31]), this implies the proposition. We then use Proposition 3.1 to prove Theorem 1.1 in the general case of Lagrangian fillings of $\lambda(\beta)$. In the specific case of $\lambda(A_{n-1})$, we obtain the following corollary.

Corollary 3.2. *The pinching sequence filling L_σ is Hamiltonian isotopic to the weave filling $L_{\mathcal{T}_\sigma}$.*

The vertical weave construction we use in the proof of Corollary 3.2 also allows us to argue that a 312-avoiding permutation yields a unique pinching sequence filling up to Hamiltonian isotopy, as we explain below. Finally, we conclude the section with a proof of Theorem 1.2 (1) as a further corollary of Theorem 1.1.

3.1. Proof of Theorem 1.1

We begin with a proof of Proposition 3.1.

Proof of Proposition 3.1. We give two local models of a D_4^- cobordism, depicted in Figures 13 and 14 as movies in the front (top) and Lagrangian (bottom) projections. The first

local model depicts the removal of a Reeb chord trapped between a pair of crossings and a 0-resolution of the rightmost crossing. The second local model depicts the removal of a Reeb chord originally appearing to the left of the leftmost crossing and a 0-resolution of this crossing. This is accomplished by first applying a Legendrian isotopy to create a pair of crossings with this Reeb chord trapped between them and proceeding as in the first local model.

The main difficulty in our comparison of these local models to the pinching cobordism is to unambiguously relate the Reeb chord removed in the D_4^- cobordism to the Reeb chord removed in the pinching cobordism. This means that we must carefully manipulate the slope of the Legendrian in the front projection to ensure that no new Reeb chords are introduced throughout the process. The local models allow us to verify by inspection that no new Reeb chords appear at any point in this cobordism, as the slopes of the front projection are specified so that no new intersections appear in the Lagrangian projection.

Armed with a local model for the slicing of the D_4^- cobordism, we now describe an exact Lagrangian isotopy between this local model and the pinching cobordism. Starting in the front projection of $\lambda(\beta)$, a slicing of the pinching cobordism as defined in Subsection 2.2.1 consists of applying the Ng resolution, resolving a crossing, and then undoing the Ng resolution. Restricting to a neighborhood of a crossing allows us to describe the desired isotopy.

First, consider a contractible Reeb chord with a neighborhood resembling one of the two models shown in Figures 13 and 14. In such a neighborhood, the exact Lagrangian isotopy between the two cobordisms is visible when examining the Lagrangian projection of the local models depicted in Figures 13 and 14 (bottom). Indeed, after applying the Ng resolution, the only difference between these local models and the pinching cobordism in the Ng resolution is the rotating of the strand before resolving. Therefore, the movie of movies realizing the exact Lagrangian isotopy from the D_4^- cobordism to the pinching cobordism consists of incrementally applying the Legendrian isotopy of the Ng resolution, rotating the crossing before pinching, and then undoing the Ng resolution.

Now consider a Reeb chord that does not admit a neighborhood resembling one of our two local models. In this case, we can rotate all of the crossings that appear to the left of the Reeb chord past the cusps by applying the local model appearing in Figure 15 so that we obtain a neighborhood resembling the initial figure in 14. We then apply the local model given in Figure 14 to resolve this crossing. Finally, we rotate the remaining crossings back, and by analogous reasoning to above, the resulting cobordism is Hamiltonian isotopic to the pinching cobordism at z.   ∎

Now that we have established the equivalence between the pinching cobordism and the D_4^- cobordism, Theorem 1.1 follows as a corollary.

Proof of Theorem 1.1. By construction, any weave filling is a decomposable Lagrangian filling made up of elementary cobordisms corresponding to Reidemeister III moves and D_4^- cobordisms. By Proposition 3.1, the D_4^- cobordism is Hamiltonian isotopic to a pinching cobordism. Therefore, a Legendrian weave filling is Hamiltonian isotopic to a decomposable Lagrangian filling made up of Reidemeister III moves and pinching cobordisms.   ∎
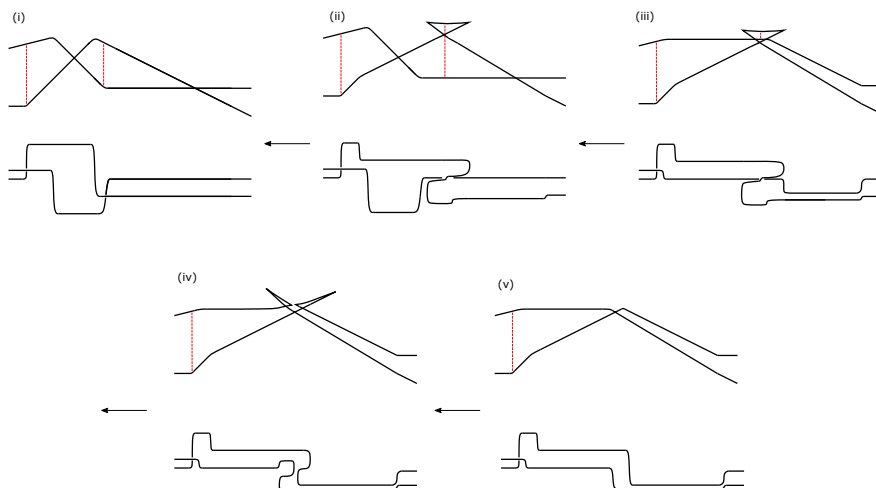
Figure 13. Local model of a D_4^- cobordism applied to a pair of crossings in the front (top) and Lagrangian (bottom) projections. Reeb chords are depicted by red dashed lines. The direction of the arrows indicate a cobordism from the concave end to the convex end.

### 3.2. Lagrangian fillings of $\lambda(A_n)$

To complete the proof of Corollary 3.2 we argue that the clip sequence bijection defined in Subsection 2.2.6 gives a one-to-one correspondence between fillings that resolves crossings in the same order.

Proof of Corollary 3.2. Let σ be a 312-avoiding permutation indexing a pinching sequence filling L_σ of $\lambda(A_{n-1})$ and consider the vertical weave corresponding to the triangulation $\mathcal{T}_\sigma$. By construction, a 0-resolution at the crossing i in $\lambda(A_{n-1})$ corresponds to a trivalent vertex where the incident rightmost edge is labeled by i. By Proposition 3.1, these denote Hamiltonian isotopic exact Lagrangian cobordisms applied to corresponding Reeb chords. Thus, the filling L_σ is Hamiltonian isotopic to the weave filling dual to the triangulation $\mathcal{T}_\sigma$. ∎

It is claimed without proof in Section 8.1 of [15] that, in addition to yielding the same Floer-theoretic invariant, there is a Hamiltonian isotopy between pinching sequence fillings represented by permutations $\sigma = \dots i\, k \dots j \dots$ and $\sigma' = \dots k\, i \dots j \dots$ in S_n. This claim implies that a 312-avoiding permutation represents a unique equivalence class of Lagrangian filling up to Hamiltonian isotopy. The claim follows from Corollary 3.2 and the lemma below.

Lemma 3.3. *Let $(x_i, z_i), (x_j, z_j)$, and (x_k, z_k) denote the coordinates of three trivalent vertices in the 2-graph Γ satisfying $x_i < x_j < x_k$ and $z_j < z_k < z_i$. The planar isotopy between Γ and the 2-graph Γ' with trivalent vertices at $(x_i, z_k), (x_j, z_j)$, and (x_k, z_i) lifts to a compactly supported Hamiltonian isotopy of the fillings L_Γ and L'_Γ fixing the boundary.*
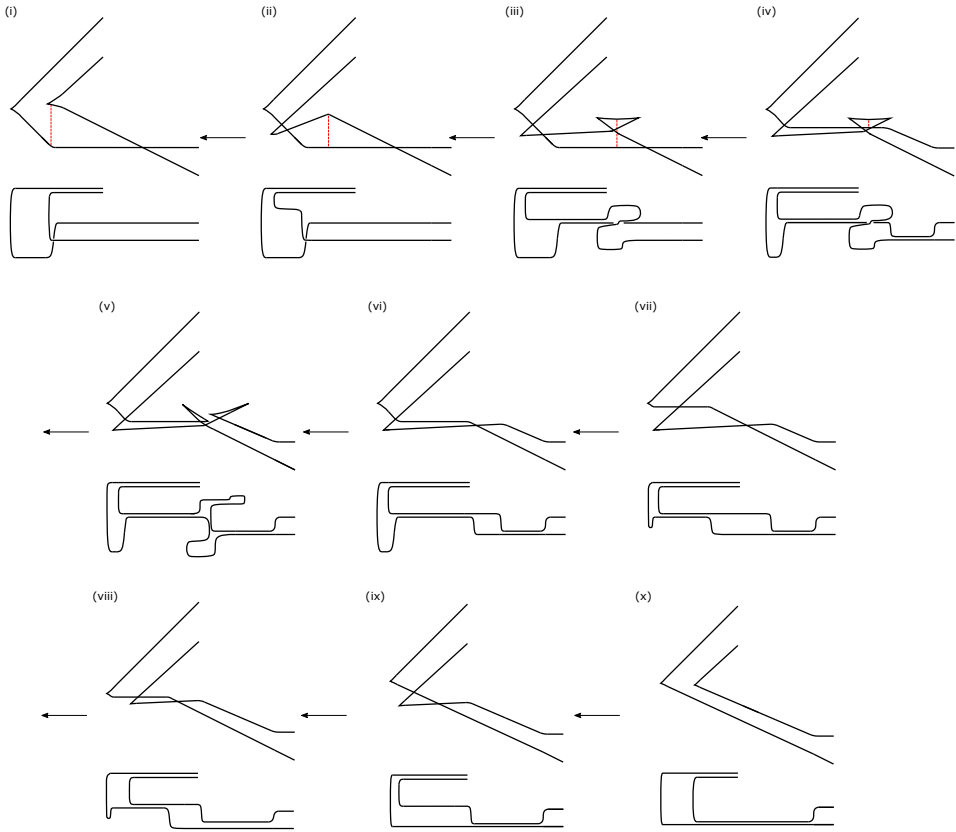
Figure 14. Local model of the leftmost crossing in the front (top) and Lagrangian (bottom) projections with a single Reeb chord depicted by a red dashed line. We first apply a Reidemeister II move in order to artificially introduce an additional crossing so that there is a single Reeb chord trapped between the new crossing and the original crossing. The D_4^- cobordism is performed in (iii)-(vi) and the remaining part of the cobordism undoes the Reidemeister II move without creating any new Reeb chords.
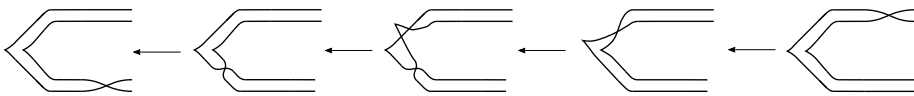
Figure 15. Local model for rotating crossings past cusps in order to isolate a desired crossing. The direction of the arrows again indicates a cobordism from the concave end to the convex end when concatenated with a cobordism described by the local model in Figure 14.

Proof. By construction, the planar isotopy between Γ and Γ' lifts to a Legendrian isotopy between the weaves $\Lambda(\Gamma)$ and $\Lambda(\Gamma')$ in $J^1(\mathbb{D}^2)$. Note that this planar isotopy can be taken to be the identity at the boundary $\partial\Lambda(\Gamma)$. Considering the Lagrangian projection of this sequence of weaves yields a compactly supported exact Lagrangian isotopy between the

Lagrangian fillings L_Γ and L'_Γ. By Theorem 3.6.7 in [31], this implies the existence of a compactly supported Hamiltonian isotopy between the two fillings.   ∎

By Corollary 3.2, the exact Lagrangian isotopy of the weave filling extends to pinching sequence fillings. Thus, our result implies that there are exactly a Catalan number C_n of pinching sequence fillings[5] of $\lambda(A_{n-1})$ up to Hamiltonian isotopy.

We conclude this section with a proof of the orbital structure described in Theorem 1.2(1) as a corollary of Theorem 1.1. Namely, the orbital structure of the Kálmán loop action on pinching sequence fillings of $\lambda(A_{n-1})$ can be obtained from the Hamiltonian isotopy between the pinching sequence filling L_σ and weave filling $L_{\mathcal{T}_\sigma}$.

Proof of Theorem 1.2(1). Let L_σ be a filling of $\lambda(A_{n-1})$ and consider the Hamiltonian isotopic weave filling $L_{\mathcal{T}_\sigma}$ with corresponding 2-graph Γ dual to the triangulation $\mathcal{T}_\sigma$. The Kálmán loop action on weave fillings is geometrically described as a cylinder rotating the entire 2-graph Γ by $2\pi/(n+2)$ radians counterclockwise. This can be readily observed from the fact that crossings of $\lambda(A_{n-1})$ are represented by edges of the dual graph intersecting the boundary of the $(n+2)$-gon. Therefore, the correspondence between triangulations $\mathcal{T}_\sigma$ and weave fillings $L_{\mathcal{T}_\sigma}$ implies that the orbital structures of triangulations under the action of rotation and weave fillings under the action of the Kálmán loop coincide. ∎

Note here the appearance of $\lambda(A_{n-1})$ as the (-1)-framed closure of the braid σ^{n+2} in the description of the weave filling. This geometrically describes why the Kálmán loop action on the rainbow closure of σ^n has order $n+2$ as an action on the $n+2$ crossings of the (-1)-framed closure.

4. Algebraic proof of Theorem 1.2

In this section we prove Theorem 1.2 by examining the Kálmán loop action on the augmentation variety $\mathrm{Aug}(\lambda(A_{n-1}))$ of the Legendrian link $\lambda(A_{n-1})$. As discussed in Subsection 2.2.2, an embedded exact Lagrangian filling yields the inclusion of an algebraic torus into the augmentation variety $\mathrm{Aug}(\lambda(A_{n-1}))$. From [30], we have an explicit computation of a set of coordinate functions $\{s_1, \ldots, s_{n-1}\}$ on an induced toric chart coming from a pinching sequence filling L; namely, this set of coordinates is in bijection with the relative cycles associated to the unstable manifolds of the saddle critical points for L. Naively, we might hope to distinguish the Hamiltonian isotopy classes of the Lagrangian fillings under the Kálmán loop action by studying the associated toric charts and their s_i coordinate functions. In practice, these *local* coordinate functions are somewhat difficult to compare under this particular action. Instead, we consider the action of the Kálmán loop on the set of *global* regular functions $\{\Delta_{i,j}\}$ with $\Delta_{i,j} \in \mathbb{Z}[\mathrm{Aug}(\lambda(A_{n-1}))]$, defined in Subsection 2.2.4. In fact, $\Delta_{i,j} \in \mathbb{Z}[z_1, \ldots, z_n]$ are globally defined polynomials, which restrict to global regular functions on the augmentation variety $\mathrm{Aug}(\lambda(A_{n-1})) \subseteq \mathbb{Z}^n$.

---

[5]Note that a precise classification of fillings currently only exists for the Legendrian unknot. In general, it is not known whether every filling is constructible, i.e., can be given as a series of elementary cobordism.

When considering the restriction of the $\Delta_{i,j}$ functions to the toric chart induced by the augmentation ε_σ, Theorem 4.1 below establishes that the correspondence between diagonals $D_{i-1,j-1}$ of the triangulation $\mathcal{T}_\sigma$ and the functions $\Delta_{i,j}$ is a $\mathbb{Z}_{n+2}$-equivariant map. We then show in Subsection 4.2 that the $\Delta_{i,j}$ functions corresponding to diagonals of a triangulation $\mathcal{T}_\sigma$ restrict to a coordinate basis of the toric chart defined by L_σ. In addition, we give an explicit formula for these coordinate functions as monomials in the s_i local coordinates. It follows the induced action on the set of augmentations ε_σ in the augmentation variety $\mathrm{Aug}(\lambda(A_{n-1}))$ is equivalent to the action of rotation on triangulations of the $(n+2)$-gon, from which we can conclude the orbital structure as given in Theorem 1.2(1). See Subsection 4.3 for a cluster-algebraic motivation for the $\Delta_{i,j}$ functions and triangulations of the $(n+2)$-gon.

4.1. The Kálmán loop action on $\{\Delta_{i,j}\}$

Let us start by describing the action of the Kálmán loop on the global regular functions $\Delta_{i,j}$ using Euler's identity for continuants. All indices in this section are modulo $n+2$. Recall that we denote by $\vartheta \in \mathrm{Aut}(\mathbb{Z}[\mathrm{Aug}(\lambda(A_{n-1}))])$ the automorphism induced by the Kálmán loop acting on the augmentation variety $\mathrm{Aug}(\lambda(A_{n-1})) = \{(z_1, \ldots, z_n) | X_n = 0\} \subseteq \mathbb{Z}^n$, where $X_n \in \mathbb{Z}[z_1, \ldots, z_n]$ is the polynomial defined by $X_n = -1 + \Delta_{1,n+2}$. The action of the Kálmán loop on the set of global regular functions $\{\Delta_{i,j}\}$ is described in the following restatement of Theorem 1.2(2).

Theorem 4.1. *The global regular functions $\Delta_{i,j}$ in $\mathbb{Z}[\mathrm{Aug}(\lambda(A_{n-1}))]$ satisfy the equation*

$$(4.1) \qquad \vartheta(\Delta_{1,k+1}) + (-1)^k \Delta_{k,n+2} = -\Delta_{2,k} X_n$$

as global polynomials in ambient $\mathbb{Z}^n$ for $2 < k < n+2$.

As a corollary, we see that the action of ϑ on the augmentation variety $\mathrm{Aug}(\lambda(A_{n-1}))$ coincides with the action of rotation on triangulations of the $(n+2)$-gon.

Corollary 4.2. *As regular functions on $\mathrm{Aug}(\lambda(A_{n-1}))$, the $\Delta_{i,j}$ satisfy*

$$\vartheta(\Delta_{i,j}) = \begin{cases} (-1)^{j-1}\Delta_{j-1,n+2} & \text{for } i = 1, \\ \Delta_{i-1,j-1} & \text{for } i \neq 1, \end{cases}$$

and the map $\Delta_{i,j} \to D_{i-1,j-1}$ is a $\mathbb{Z}_{n+2}$-equivariant map.

Proof of Corollary 4.2. The case of $i > 1$ is discussed in Subsection 2.2.6, and follows from the formula for $\vartheta(\Delta_{i,j})$ given there. In the case of $i = 1$, restricting to $\mathrm{Aug}(\lambda(A_{n-1}))$ $= \{X_n = 0\}$ causes the right-hand side of equation (4.1) to vanish. Therefore, by Theorem 4.1, the Kálmán loop action on the restriction of $\Delta_{1,j}$ to $\mathrm{Aug}(\lambda(A_{n-1}))$ is $\vartheta(\Delta_{1,j}) = (-1)^j \Delta_{j-1,n+2}$. Under rotation, the diagonal $D_{i-1,j-1}$ maps to $D_{i-2,j-2}$. It follows that the correspondence between $\Delta_{i,j}$ restricted to the toric chart induced by ε_σ and a diagonal $D_{i-1,j-1}$ of the triangulation $\mathcal{T}_\sigma$ is a $\mathbb{Z}_{n+2}$-equivariant map. ∎

We now give a proof of the behavior of the $\Delta_{i,j}$ as ambient polynomials in $\mathbb{Z}^n$. Note here the appearance of Euler's identity for continuants in the form of equation (2.2).

Proof of Theorem 4.1. We first rewrite the left-hand side of the desired equation using the continuant recursion relation (2.1) and the action of ϑ:

$$\vartheta(\Delta_{1,k+1}) + (-1)^{k-1}\Delta_{k,n+2} = \vartheta(z_1\Delta_{2,k+1} + \Delta_{3,k+1}) + (-1)^{k-1}\Delta_{k,n+2}$$
$$= -\Delta_{2,n+2}\,\Delta_{1,k} + \Delta_{2,k} + (-1)^{k-1}\Delta_{k,n+2}.$$

We substitute this expression into the left-hand side of the desired equation from Theorem 4.1 to obtain

$$-\Delta_{2,n+2}\,\Delta_{1,k} + \Delta_{2,k} + (-1)^{k-1}\Delta_{k,n+2} = -\Delta_{2,k}(\Delta_{1,n+2} - 1).$$

In order to verify that this equation holds, we will apply the special case of Euler's identity for continuants given in equation (2.2). To do so, we distribute the right-hand side and subtract $\Delta_{2,k}$ from both sides to get

$$-\Delta_{2,n+2}\Delta_{1,k} + (-1)^{k-1}\Delta_{k,n+2} = -\Delta_{2,k}\,\Delta_{1,n+2}.$$

This expression is equivalent to

$$\Delta_{1,n+2}\,\Delta_{2,k} - \Delta_{1,k}\,\Delta_{2,n+2} = (-1)^k\,\Delta_{k,n+2},$$

which is the identity given in equation (2.2). Thus, we have established Theorem 4.1 and Theorem 1.2(2). ∎

4.2. The Kálmán loop action on the augmentation variety

We now prove that the $\Delta_{i,j}$ functions corresponding to the diagonals of the triangulation $\mathcal{T}_\sigma$ define a coordinate basis on the toric chart induced by the filling L_σ. To do so, we first show that the $\Delta_{i,j}$ functions can be written as monomials in the local s_i coordinate functions defined by the augmentation ε_σ. We then define a bijection between the $\Delta_{i,j}$ corresponding to the triangulation $\mathcal{T}_\sigma$ and the s_i variables on the toric chart induced by L_σ. Throughout the remainder of this section, let σ denote a 312-avoiding permutation corresponding to a pinching sequence filling and $D_{i,j}$ be a diagonal of the triangulation $\mathcal{T}_\sigma$. The goal of this subsection will be to prove the following proposition.

Proposition 4.3. *The set of all $\Delta_{i,j}$ corresponding to the diagonals of the triangulation $\mathcal{T}_\sigma$ forms a basis for the toric chart induced by the augmentation ε_σ.*

The technical lemma introduced below will be used to prove the first part of Proposition 4.3.

Lemma 4.4. *For any diagonal $D_{i-1,j-1}$ in the triangulation $\mathcal{T}_\sigma$, the image of the regular function $\Delta_{i,j}$ in the toric chart induced by the augmentation ε_σ is given by $\varepsilon_\sigma(\Delta_{i,j}) = s_i \ldots s_{j-2}$.*

Assuming the lemma, we first prove Proposition 4.3.

Proof of Proposition 4.3. We first define a bijection φ between the set of triangles in the triangulation $\mathcal{T}_\sigma$ and the local toric coordinates $s_1, \ldots, s_{n-1}$ induced by the augmentation ε_σ. Let T be a triangle in $\mathcal{T}_\sigma$ with sides $D_{i-1,j-1}, D_{j-1,k-1}$ and $D_{i-1,k-1}$. We define

the map φ by

$$\varphi(T) := (\Delta_{i,j})^{-1}(\Delta_{j,k})^{-1}\Delta_{i,k}.$$

where we recall that $\Delta_{i,i+1} = 1$ by definition. By Lemma 4.4, we have

$$(\Delta_{i,j})^{-1}(\Delta_{j,k})^{-1}\Delta_{i,k} = (s_i \ldots s_{j-2})^{-1}(s_j \ldots s_{k-2})^{-1}s_i \ldots s_{k-2} = s_{j-1}.$$

To see that φ is injective, consider two triangles T and T' belonging to the triangulation $\mathcal{T}_\sigma$ with sides $\{D_{i-1,j-1}, D_{j-1,k-1}, D_{i-1,k-1}\}$ and $\{D_{i'-1,j'-1}, D_{j'-1,k'-1}, D_{i'-1,k'-1}\}$, respectively. Assume that $\varphi(T) = \varphi(T')$. Then $s_{j-1} = s_{j'-1}$, and therefore $j = j'$. Since the triangles T and T' share a middle vertex, and belong to the same triangulation, they must be the same. We conclude immediately that φ is bijective because it is an injective map between two sets of $n-1$ elements. Thus, the set of $\Delta_{i,j}$ functions corresponding to diagonals $\mathcal{T}_\sigma$ form a coordinate basis for the toric chart induced by the augmentation ε_σ. ∎

We now give a proof of Lemma 4.4 by carefully examining the effect of the DGA map Φ on the braid matrices defining $\Delta_{i,j}$.

Proof of Lemma 4.4. Consider $\Delta_{i,j}$ corresponding to some diagonal $D_{i-1,j-1}$ of a triangulation $\mathcal{T}_\sigma$. By definition, we have

$$\Phi(\Delta_{i,j}) = \Big[\prod_{k=i}^{j-2} B(\Phi(z_k))\Big]_{(2,2)}.$$

Therefore, Lemma 4.4 is equivalent to the claim that the $(2,2)$ entry of $\prod_{k=i}^{j-2} B(\varepsilon_\sigma(z_k))$ is precisely $\prod_{k=i}^{j-2} s_k$.

To verify this statement, we show inductively that applying $\Phi_l \circ \cdots \circ \Phi_1$ yields a product of $B(z_k)$ for $k \in \{i, \ldots, j-2\}\backslash\{\sigma(1), \ldots, \sigma(l)\}$ with a particular collection of diagonal matrices, upper triangular and lower triangular matrices.

Define the matrices

$$C(s) := \begin{pmatrix} 1 & s \\ 0 & 1 \end{pmatrix}, \quad U(s) := \begin{pmatrix} -s^{-1} & 1 \\ 0 & s \end{pmatrix}, \quad Ł(s) := \begin{pmatrix} -s^{-1} & 0 \\ 1 & s \end{pmatrix}, \quad D(s) := \begin{pmatrix} -s^{-1} & 0 \\ 0 & s \end{pmatrix}.$$

Denote by A^T the transpose of the matrix A. The following identities are immediate:

$$(4.2) \qquad\qquad B(z \pm s) = B(z)\,C(\pm s),$$

$$(4.3) \qquad\qquad B(z \pm s) = C^\mathsf{T}(\pm s)\,B(z),$$

$$(4.4) \qquad\qquad C(s \pm t) = C(s)\,C(\pm t),$$

$$(4.5) \qquad C(-s^{-1})\,B(s)\,C^\mathsf{T}(-s^{-1}) = D(s),$$

$$(4.6) \qquad\qquad C(-s^{-1})\,B(s) = L(s),$$

$$(4.7) \qquad\qquad B(s)\,C^\mathsf{T}(-s^{-1}) = U(s).$$

Equipped with this set of identities, we proceed with the proof of Lemma 4.4. First, we may assume that $\sigma(1), \ldots, \sigma(k)$ all lie in the set $\{i, \ldots, j-2\}$. Indeed, for $\sigma(l)$ not

in $\{i, \ldots, j-2\}$, the map Φ_l is the identity on the polynomial $\Phi_{l-1} \circ \cdots \circ \Phi_1(\Delta_{i,j})$. This follows from the observation that if $D_{i-1,j-1}$ is in the triangulation $\mathcal{T}_\sigma$, then i appears before $i-1$ and $j-2$ appears before $j-1$ in σ under the clip sequence bijection. Therefore, $\sigma^{-1}(i) < \sigma^{-1}(i-1)$ and $\sigma^{-1}(j-2) < \sigma^{-1}(j-1)$, which implies that no elements of the set T_σ^l appear in terms of $\Phi_{l-1} \circ \cdots \circ \Phi_1(\Delta_{i,j})$.

We denote by M_l^+ and M_l^- the maximum and minimum of the set $\{i, \ldots, j-2\} \setminus \{\sigma(1), \ldots, \sigma(l-1)\}$. We claim that the result of applying Φ_l to $\Phi_{l-1} \circ \cdots \circ \Phi_1(\Delta_{i,j})$ results in the replacement of $B(z_{\sigma(l)})$ in the product $\prod_{k=i}^{j-2} B(\Phi_{l-1} \circ \cdots \circ \Phi_1(z_k))$ with one of three possibilities depending on l:

(1) For $\sigma(l) = M_l^-$, the map Φ_l replaces $B(z_{\sigma(l)})$ by the upper triangular matrix $U(s_{\sigma(l)})$.
(2) For $\sigma(l) = M_l^+$, the map Φ_l replaces $B(z_{\sigma(l)})$ by the lower triangular matrix $L(s_{\sigma(l)})$.
(3) For $M_l^- < \sigma(l) < M_l^+$, the map Φ_l replaces $B(z_{\sigma(l)})$ by the diagonal matrix $D(s_{\sigma(l)})$.

We prove this claim by induction. For the base case, we consider the three possibilities listed above.

Case (1). If $\sigma(1) = M_1^- = i$, then we have

$$\Phi_1(\Delta_{i,j}) = B(s_i) B(z_{i+1} - s_i^{-1}) B(z_{i+2}) \ldots B(z_{j-2})$$
$$= B(s_i) C^\top(-s_i^{-1}) B(z_{i+1}) \ldots B(z_{j-2}) = U(s_i) B(z_{i+1}) \ldots B(z_{j-2}),$$

where the second equality follows from (4.3), and the final one from (4.7).

Case (2). If $\sigma(1) = M_1^+ = j-2$, then equations (4.2) and (4.6) imply that

$$\Phi_1(\Delta_{i,j}) = B(z_i) \ldots B(z_{j-3}) C(-s_{j-2}^{-1}) B(s_{j-2}) = B(z_i) \ldots B(z_{j-3}) L(s_{j-2}).$$

Case (3). If $i < \sigma(1) < j-2$, then we apply equations (4.2), (4.3), and (4.5) to $\Phi_1(\Delta_{i,j})$ to obtain

$$\Phi_1(\Delta_{i,j}) = B(z_i) \ldots B(z_{\sigma(1)-1}) C(-s_{\sigma(1)}^{-1}) B(s_{\sigma(1)}) C^\top(-s_{\sigma(1)}^{-1}) B(z_{\sigma(1)+1}) \ldots B(z_{j-2})$$
$$= B(z_i) \ldots B(z_{\sigma(1)-1}) D(s_{\sigma(1)}) B(z_{\sigma(1)+1}) \ldots B(z_{j-2}).$$

Assume inductively that applying the composition $\Phi_{l-1} \circ \cdots \circ \Phi_1$ replaces, for $1 \leq k \leq l-1$, each $B(z_{\sigma(k)})$ with either $U(s_{\sigma(k)})$, $L(s_{\sigma(k)})$, or $D(s_{\sigma(k)})$ depending on whether $\sigma(k) = M_k^-$, $\sigma(k) = M_k^+$, or $M_k^- < \sigma(k) < M_k^+$, respectively. We consider the same three cases for Φ_l.

Case (1). If $\sigma(l) = M_l^-$, then T_σ^l has a single element l' and by the combinatorial formula for Φ_l, we have

$$B(\Phi(z_{\sigma(l')})) = C^\top(\pm s_{\sigma(l)}^{-1} s_{\sigma(l)+1}^{-2} \ldots s_{\sigma(l')-1}^{-2}) B(z_{\sigma(l')}),$$

where the sign is given by $(-1)^{|\sigma(l)-(\sigma(l')-1)|}$. By the inductive hypothesis, we have that the matrices appearing between $B(\Phi(z_{\sigma(l)})) = B(s_{\sigma(l)})$ and $C^\top(s_{\sigma(l)}^{-1} s_{\sigma(l)+1}^{-2} \ldots s_{\sigma(l')-1}^{-2})$

are of the form $D(s_{\sigma(l)+1}) \ldots D(s_{\sigma(l')-1})$. We then compute the product

$$B(s_{\sigma(l)}) \left(\prod_{m=\sigma(l)+1}^{\sigma(l')-1} D(s_m) \right) C^{\mathsf{T}}(\pm s_{\sigma(l)}^{-1} s_{\sigma(l)+1}^{-2} \cdots s_{\sigma(l')-1}^{-2}),$$

which simplifies to

$$\begin{pmatrix} \pm s_{\sigma(l)}^{-1} \cdots s_{\sigma(l')-1}^{-1} & s_{\sigma(l)+1} \cdots s_{\sigma(l')-1} \\ 0 & s_{\sigma(l)} \cdots s_{\sigma(l')-1} \end{pmatrix} = U(s_{\sigma(l)}) \left(\prod_{m=\sigma(l)+1}^{\sigma(l')-1} D(s_m) \right),$$

showing that applying Φ_l replaces $B(z_l)$ by $U(s_l)$.

Case (2). If $\sigma(l) = M_l^+$, then T_σ^l again has a single element l'' and we have

$$C(\pm s_{\sigma(l'')+1}^{-2} \cdots s_{\sigma(l)-1}^{-2} s_{\sigma(l)}^{-1}) \left(\prod_{m=\sigma(l'')+1}^{\sigma(l)-1} D(s_m) \right) B(s_{\sigma(l)}) = \left(\prod_{m=\sigma(l'')+1}^{\sigma(l)-1} D(s_m) \right) L(s_{\sigma(l)}).$$

Case (3). Finally, if $M_l^- < \sigma(l) < M_l^+$, then T_σ^l has two elements, denote them by l' and l'' with $l' > l''$. Then we must consider the product of

$$C(\pm s_{\sigma(l'')+1}^{-2} \cdots s_{\sigma(l)-1}^{-2} s_{\sigma(l)}^{-1}) \left(\prod_{m=\sigma(l'')+1}^{\sigma(l)-1} D(s_m) \right)$$

with

$$B(s_{\sigma(l)}) \left(\prod_{m=\sigma(l)+1}^{\sigma(l')-1} D(s_m) \right) C^{\mathsf{T}}(\pm s_{\sigma(l)}^{-1} s_{\sigma(l)+1}^{-2} \cdots s_{\sigma(l')-1}^{-2})$$

where the two signs of entries of C and C^{T} need not agree. We apply our computation from the previous case and simplify

$$\left(\prod_{m=\sigma(l'')+1}^{\sigma(l)-1} D(s_m) \right) L(s_{\sigma(l)}) \left(\prod_{m=\sigma(l)+1}^{\sigma(l')-1} D(s_m) \right) C^{\mathsf{T}}(\pm s_{\sigma(l)}^{-1} s_{\sigma(l)+1}^{-2} \cdots s_{\sigma(l')-1}^{-2})$$

$$= \left(\prod_{m=\sigma(l'')+1}^{\sigma(l)-1} D(s_m) \right) L(s_{\sigma(l)}) \begin{pmatrix} \mp (s_{\sigma(l)+1} \cdots s_{\sigma(l')-1})^{-1} & 0 \\ \pm (s_{\sigma(l)} s_{\sigma(l)+1} \cdots s_{\sigma(l')-1})^{-1} & s_{\sigma(l)+1} \cdots s_{\sigma(l')-1} \end{pmatrix}.$$

This yields the product

$$\prod_{m=\sigma(l'')+1}^{\sigma(l')-1} D(s_m),$$

as desired.

Thus, by induction, Φ_l replaces $B(z_l)$ with an upper triangular, lower triangular, or diagonal matrix for $1 < l < j - 2 - i$. Therefore, when we arrive at the final Φ_{j-2-i} map,

we have $B_{s_{\sigma(j-2-i)}}$ multiplied on the left by the product of some number of upper triangular and diagonal matrices with the corresponding s variable appearing in the $(2, 2)$ entry and multiplied on the right by some number of diagonal and lower triangular matrices with the same condition. Since multiplication by a diagonal matrix preserves the property of being upper or lower triangular, the result is a product of the form $UB(s_{\sigma(j-2-i)})L$, where U and L are upper and lower triangular matrices. Therefore, the $(2, 2)$ entry of this product is the product of the $(2, 2)$ entries of each of the factors. It follows that the $(2, 2)$ entry of $\Phi(\Delta_{i,j})$ is $s_i \ldots s_{j-2}$, as desired.   ∎

Together, Corollary 4.2 and Proposition 4.3 allow us to give an algebraic proof of Theorem 1.2(1).

Proof of Theorem 1.2(1). By Proposition 4.3, the set of $\Delta_{i,j}$ corresponding to a triangulation $\mathcal{T}_\sigma$ gives a basis for the toric chart induced by the augmentation ε_σ. Therefore, the image of ε_σ under ϑ corresponds to the image of the set of $\Delta_{i,j}$ corresponding to $\mathcal{T}_\sigma$. By Corollary 4.2, we know that the induced action of the Kálmán loop on the augmentation variety of $\lambda(A_{n-1})$ is equivalent to the action of rotation on the $(n + 2)$-gon. Therefore, the orbital structure of the action can be described as in Subsection 2.3.2.   ∎

4.3. Relation to cluster theory

The appearance of the $\Delta_{i,j}$ functions and the combinatorics of the $(n + 2)$-gon is explained by a cluster structure on the augmentation variety, the existence of which was recently proven by Gao–Shen–Weng in [23]. In brief, a cluster variety is an algebraic variety containing a set of toric charts (cluster charts) with coordinate functions (cluster variables) that transform according to a specific operation (cluster mutation) under the chart maps. See [19, 20] for more on cluster algebras.

For a Legendrian λ given as the rainbow closure of a positive braid, [23] describes a cluster structure on $\mathrm{Aug}(\lambda)$ by proving a natural isomorphism to double Bott–Samelson cells. In particular, the cluster structure on $\mathrm{Aug}(\lambda(A_{n-1}))$ is a cluster algebra of A-type. A-type cluster algebras were originally defined and studied by Fomin and Zelevinksy in the context of regular functions on the affine cone of the Grassmanian $\mathscr{G}r^\times(2, n + 2)$, see [21]. If we consider the Plücker coordinate $P_{i,j}$ of the (ordinary) Grassmanian $\mathrm{Gr}(2, n + 2)$, then its image in the affine cone is precisely the function $\Delta_{i,j}$. The combinatorics of the relationship between cluster charts is captured by the flip graph, where a single cluster seed is given by all $\Delta_{i,j}$ corresponding to diagonals $D_{i,j}$ of a triangulation. In the context of this manuscript, [23] implies the existence of cluster coordinates on $\mathrm{Aug}(\lambda(A_{n-1}))$, while Proposition 4.3 gives a precise formula.

Also of interest in the cluster setting is the fact that the Kálmán loop induces a cluster automorphism of the augmentation variety $\mathrm{Aug}(\lambda(A_{n-1}))$. Subsection 5.2 explicitly realizes this automorphism as a sequence of mutations. For an A-type cluster algebra, Assem, Schiffler, and Shramchenko showed [3] that the cluster automorphism group is $\mathbb{Z}_{n+2}$. Theorem 4.1 implies that the order of the Kálmán loop action on $\mathrm{Aug}(\lambda(A_{n-1}))$ is precisely $n + 2$, so we immediately deduce the following corollary.

Corollary 4.5. *The induced action of the Kálmán loop on* $\mathrm{Aug}(\lambda(A_{n-1}))$ *is a generator of the A-type cluster modular group.*

5. Combinatorial characterizations

In this section, we describe the combinatorial properties of the Kálmán loop action on a pinching sequence filling L_σ of $\lambda(A_{n-1})$ purely in terms of the corresponding 312-avoiding permutation σ. We first present an explicit algorithm for determining the orbit size of L_σ from σ in Subsection 5.1. The end of the subsection includes a table where orbit sizes are computed for the case $n = 4$, corresponding to triangulations of the hexagon. We then give a recipe for constructing a geodesic path in the flip graph that describes a counterclockwise rotation of the triangulation $\mathcal{T}_\sigma$. Since the weave filling $L_{\mathcal{T}_\sigma}$ is Hamiltonian isotopic to the pinching sequence filling L_σ by Theorem 1.1, this geodesic path describes the Kálmán loop action on L_σ as a sequence of edge flips. Finally, we discuss the behavior of 312-avoiding permutations under a single edge flip in the flip graph. Together, these last two results give a combinatorial characterization of the Kálmán loop action on fillings purely in terms of 312-avoiding permutations. As in previous sections, all indices are computed modulo $n + 2$.

5.1. Orbit size

To prove Theorem 1.3, we give explicit criteria in Lemmas 5.4 and 5.5 for when a filling of $\lambda(A_{n-1})$ has orbit size $(n + 2)/2$ or $(n + 2)/3$ under the action of the Kálmán loop. If it does not satisfy either of these criteria, then it necessarily has orbit size $n + 2$. We start by describing the permutations that arise from an orbit of size $(n + 2)/2$.

Consider some 312-avoiding permutation $\sigma \in S_n$. In order for the filling L_σ to have orbit size $(n + 2)/2$, the triangulation $\mathcal{T}_\sigma$ must have rotational symmetry through an angle of π. Therefore, $\mathcal{T}_\sigma$ has a diameter $D_{i,i+(n+2)/2}$ and the triangulated polygons on either side of this diameter must be mirror images. We consider the diameter as an external edge of two $(\frac{n+2}{2} + 1)$-gons, one containing both vertices labeled $n + 1$ and $n + 2$, and the other containing at most one of them. For any 312-avoiding permutation σ such that $\mathcal{T}_\sigma$ has a diameter $D_{i,i+(n+2)/2}$, we define the 312-avoiding permutation τ in $S_{(n+2)/2}$ corresponding to half of the triangulation $\mathcal{T}_\sigma$ as follows.

Definition 5.1. The permutation τ in the letters $i + 1, i + 1, \ldots, i + (n + 2)/2 - 1$ is the 312-avoiding permutation obtained from applying the clip sequence bijection to the triangulation $\mathcal{T}_\tau$ of the $(\frac{n+2}{2} + 1)$-gon containing at most one of the vertices labeled by $n + 1$ and $n + 2$.

We can always unambiguously identify τ from the permutation σ.

Lemma 5.2. *Let $\sigma \in S_n$ be any 312-avoiding permutation such that $\mathcal{T}_\sigma$ has rotational symmetry through an angle of π. The permutation τ is the first subword of σ of length $n/2$ letters forming a subinterval of the integers $\{1, \ldots, n\}$.*

Proof. Let $\sigma \in S_n$ correspond to a triangulation $\mathcal{T}_\sigma$ with rotational symmetry through an angle of π. Under the clip sequence bijection, there may be letters of σ that appear before τ. Therefore, to identify τ as a subword of σ, we search for the first 312-avoiding permutation of length $n/2$ that appears in σ. A diameter $D_{i,i+(n+2)/2}$ forces the condition that any letters appearing before τ will be less than i, so that even if i appears directly after τ, there is no ambiguity in identifying τ.

Explicitly, we identify τ by first checking if the set $\{\sigma(1), \dots \sigma(n/2)\}$ of the first $n/2$ letters of σ is equal to a subinterval of the integers $\{1, \dots, n\}$ of length $n/2$. If not, we check the $\{\sigma(2), \dots, \sigma(n/2+1)\}$. We continue in this way until we have either identified the subword τ or exhausted all possibilities. If no such subword exists, then σ does not have the assumed rotational symmetry. ∎

We now state a preparatory lemma regarding details of the clip sequence bijection that may give some insight into the structure of the orbit size algorithm below. We consider the most general case where $\mathcal{T}_\tau$ is a subtriangulation of $\mathcal{T}_\sigma$ with vertices $i, \dots, i+k$ for $i+k \le n+1$.

Lemma 5.3. *Let $k \in \mathbb{N}$ satisfy $j < i + k \le n + 1$. The 312-avoiding permutation τ ends in the letter j if and only if the subtriangulation $\mathcal{T}_\tau$ contains the triangle labeled by vertices i, j, and $i + k$. In this case, all letters taking values strictly between i and j appear before any other letters in τ.*

Proof. The first claim follows from the definition of the clip sequence bijection because the diagonal $D_{i,i+k}$ must appear in the final triangle remaining after removing the previous $n-1$ vertices. Therefore, j is the final letter of τ if and only if it is also the third vertex of this triangle.

The second claim follows by similar reasoning to the case of the diameter, as the existence of the diagonal $D_{i,j}$ implies that there must be some ear $D_{l,l+2}$ with $i < l < j - 2$. Therefore, $l + 1$ appears before j and we can repeat this argument for the subtriangulation of $\mathcal{T}_\tau$ obtained by removing the vertex $l + 1$. ∎

We now give explicit criteria for determining whether the filling L_σ has orbit size $(n+2)/2$ solely in terms of σ.

Lemma 5.4. *The following algorithm detects whether a 312-avoiding permutation σ in S_n yields a filling L_σ of orbit size $(n+2)/2$ under the action of the Kálmán loop.*

(1) Identify τ from σ as in the proof of Lemma 5.2.

(2) Define σ' to be an empty string and set $\tau' = \tau$. Find the smallest j for which $j \ge \frac{n+2}{2}$ and some $k > j$ appears before j in τ. For the first such k appearing in τ', append $k - \frac{n+2}{2}$ to σ', remove k from τ' and repeat until no such letters remain in τ'. Append τ to σ'.

(3) While τ' ends in the largest (respectively, smallest) number remaining in τ' not equal to $\frac{n+2}{2} - 1$ (respectively, $\frac{n+2}{2}$), then append the next largest (respectively, next smallest) number in $\{1, \dots, n\} \backslash \sigma'$ less than the smallest number (respectively, greater than the largest number) of τ' to σ' and delete the final number of τ'.

(4) If τ' does not end in its largest or smallest remaining number, then add $\frac{n+2}{2}$ to all numbers less than the final number and append to σ' in the order they appear. Delete the corresponding numbers from τ'.

(5) Now τ' ends in its smallest remaining number, so return to Step (3) and repeat until only one number remains in τ'. The final number of σ' is then determined by the unique number remaining in $\{1, \dots, n\} \backslash \sigma'$.

(6) σ has orbit size $\frac{n+2}{2}$ if it is equal to σ'.

Example. Consider the 312-avoiding permutation $\sigma = 154362$. We can identify $\tau = 543$ as the first length 3 subword appearing in σ and the diameter of the triangulation $\mathcal{T}_\sigma$ is therefore $D_{2,6}$. Applying the above algorithm to τ, we see that Step (2) yields $\sigma' = 1543$, because 5 precedes 4. Then 3 is the smallest number appearing in τ, so we append 6 to σ'. Finally, we append 2, to get $\sigma = \sigma'$, indicating that the filling labeled by σ has orbit size 4 under the Kálmán loop.

Proof of Lemma 5.4. Let $\sigma \in S_n$ be a 312-avoiding permutation with orbit size $\frac{n+2}{2}$. Denote the diameter of $\mathcal{T}_\sigma$ as $D_{i,i+(n+2)/2}$ for some $1 \leq i \leq \frac{n+2}{2} - 1$, and call τ the permutation corresponding to the triangulation of the $(\frac{n+2}{2} + 1)$-gon given by the vertices $i, \ldots, i + \frac{n+2}{2}$. We will show that the algorithm detects when the triangulation $\mathcal{T}_\sigma$ is obtained from the triangulation $\mathcal{T}_\tau$ by gluing $\mathcal{T}_\tau$ to a rotation of $\mathcal{T}_\tau$ by π along the diagonal $D_{i,i+(n+2)/2}$. The lemma then follows from the observation that τ is uniquely determined from σ.

Under the clip sequence bijection, we delete the smallest vertex with no incident diagonal at each step and append the label to the permutation. Therefore, any letter k of σ appearing before τ is less than i. Moreover, any diagonal $D_{j,k}$ or $D_{k,j}$ (should it exist) incident to the vertex k has endpoint j in the set $\{n + 2, 1, \ldots, i\}$. Therefore any triangle with vertices j, k,and l with j, k, l given in clockwise order must also have $j, l \in \{n + 2, 1, \ldots, i\}$. The rotational symmetry of $\mathcal{T}_\sigma$ implies that the triangle with vertices $j + \frac{n+2}{2}, k + \frac{n+2}{2}, l + \frac{n+2}{2}$ appears in $\mathcal{T}_\tau$. It follows from Lemma 5.3 that in τ the letter $k + \frac{n+2}{2}$ precedes j for some $j \geq \frac{n+2}{2}$ and that all such k appear before τ in σ. Therefore, Step (2) produces all letters of σ that appear before τ.

To determine the letters following τ in σ, we first consider the case where one of the diameter vertices, i or $i + \frac{n+2}{2}$, has no incident diagonals with endpoint taking values in the set of vertices labeled by letters appearing after τ in σ. If this is the case, then the appropriate diameter vertex label immediately follows τ in σ under the clip sequence bijection. We also observe that when i (respectively, $i + \frac{n+2}{2}$) is such a vertex, then there is a triangle in $\mathcal{T}_\sigma$ with vertices $i, i - 1$, and $i + \frac{n+2}{2}$ (respectively, $i, i + \frac{n+2}{2}, i + \frac{n+2}{2} + 1$). Therefore, the rotational symmetry of $\mathcal{T}_\sigma$ implies that we have a triangle with vertices $i, i + \frac{n+2}{2} - 1$ and $i + \frac{n+2}{2}$ (respectively, $i, i + 1$, and $i + \frac{n+2}{2}$) in $\mathcal{T}_\tau$. By Lemma 5.3, the vertex $i + \frac{n+2}{2} - 1$ (respectively, $i + 1$) appears as the final letter in τ. The vertex $i - 1$ (respectively, $i + \frac{n+2}{2} + 1$) then appears immediately following τ. The same reasoning applies if we replace the diameter $D_{i,i+(n+2)/2}$ with the diagonal $D_{i-1,i+(n+2)/2}, D_{i,i+(n+2)/2+1}$, or any such longest remaining diagonal arising under the clip sequence bijection in this way, so long as $n + 1$ or $n + 2$ do not appear as endpoints of this diagonal.

If both diameter vertices have diagonals incident to them with endpoints in the remaining vertices, then the letter following τ under the clip sequence bijection labels the smallest vertex greater than $i + \frac{n+2}{2}$ with no incident diagonals. By previous reasoning, we know that the diameter is one side of a triangle with vertices $i, k, i + \frac{n+2}{2}$ in $\mathcal{T}_\sigma$. The rotational symmetry of $\mathcal{T}_\sigma$ implies that the triangle labeled by $i, k - \frac{n+2}{2}, i + \frac{n+2}{2}$ appears in $\mathcal{T}_\tau$. It follows from Lemma 5.3 that $k - \frac{n+2}{2}$ appears as the final letter of τ, and that any letters j with $j < k - \frac{n+2}{2} < \frac{n+2}{2}$ appearing before $k - \frac{n+2}{2}$ in τ correspond to let-

ters $j + \frac{n+2}{2}$ appearing in order following τ. After these vertices are deleted by the clip sequence bijection, $k - \frac{n+2}{2}$ is now the smallest remaining letter in τ.

This process continues until we have eliminated all numbers from τ except for either $n + 1$ or $n + 2$. This unambiguously determines the final number of our permutation. By construction, we have shown that the above algorithm yields the 312-avoiding permutation σ with $\mathcal{T}_\sigma$ constructed by gluing a rotated copy of $\mathcal{T}_\tau$ to $\mathcal{T}_\tau$. ∎

We now consider the case of a 312-avoiding permutation σ with orbit size $\frac{n+2}{3}$. In order to exhibit the appropriate rotational symmetry, the triangulation $\mathcal{T}_\sigma$ must have a central triangle labeled by vertices $i, i + \frac{n+2}{3}, i + \frac{2(n+2)}{3}$, dividing the triangulation up into three identical triangulations of $(\frac{n+2}{3} + 1)$-gons. Two of these polygons do not contain the pair of vertices $n + 1$ and $n + 2$, so a permutation σ with $\mathcal{T}_\sigma$ having rotational symmetry through an angle of $\frac{2\pi}{3}$ must have two subwords τ_1 and τ_2 of length $\frac{n+2}{3} - 1$ that differ by $\frac{n+2}{3}$ and are immediately followed by $i + \frac{n+2}{3}$. We determine the third subword from τ_1 using the same reasoning as in the $\frac{n+2}{2}$ orbit size case.

Lemma 5.5. *The following algorithm detects whether a 312-avoiding permutation σ in S_n yields a filling L_σ of orbit size $(n + 2)/3$ under the action of the Kálmán loop.*

(1) Determine τ_1 by finding the first subword of length $\frac{n+2}{3} - 1$ in σ with letters $i, \ldots,$ $i + \frac{n+2}{3} - 1$ for some i. If no such τ_1 exists, then σ does not have orbit size $\frac{n+2}{3}$.

(2) Set σ' to be the empty word. For any numbers greater than $\frac{n+2}{3}$ that appear after $\frac{n+2}{3}$ or some other number greater than $\frac{n+2}{3}$, add $\frac{2(n+2)}{3}$ (mod $n + 2$) to them and append the result to σ'. Append τ_1 to σ'. Add $\frac{n+2}{3}$ to each entry of τ_1 to get τ_2 and append to σ'. Append $i + \frac{n+2}{3}$ to σ'. Delete the corresponding number from τ_1.

(3) So long as τ_1 ends in the largest (respectively, smallest) number remaining in τ_1 not equal to $\frac{n+2}{3} - 1$ (respectively, $\frac{n+2}{3}$), then append the next largest (respectively, next smallest) number of $\{1, \ldots, n\} \backslash \sigma'$ less than the smallest number (respectively, greater than the largest number) of τ_1 to σ' and delete the final number in τ_1.

(4) If τ_1 does not yet end in the largest or smallest remaining number, add $\frac{n+2}{3}$ to all numbers less than the final number and append. Delete the corresponding numbers from τ_1.

(5) Now τ_1 ends in the smallest remaining number, so return to Step (3) and continue until one number remains in τ_1. The final number of σ' is then determined by the unique number appearing in $\{1, \ldots, n\} \backslash \sigma'$.

(6) σ has orbit size $\frac{n+2}{3}$ if it is equal to σ'.

Example. We can identify $\sigma = 2\,1\,5\,4\,3\,6\,7$ as a permutation with orbit size $(7 + 2)/3 = 3$ using the above algorithm. First identify τ_1 as the first length 2 subword with two consecutive letters, i.e., $\tau_1 = 2\,1 \in S_2$. Then $\tau_2 = 5\,4$ and the string $2\,1\,5\,4\,3$ must appear in σ in order for it to have orbit size 3. We can also determine that no letters appear before τ_1 because 1 and 2 already appear in our word. Since τ_1 ends with the smallest letter of the triangulation $\mathcal{T}_{\tau_1}$, we append 6. The final remaining number is 7, so we see that $\sigma' = \sigma$ and therefore σ has orbit size 3.

We conclude this subsection with a table of orbit sizes of pinching sequence fillings of $\lambda(A_3)$, i.e., the case $n = 4$.

Permutation	Orbit size
1 2 3 4	6
1 2 4 3	3
1 3 2 4	2
1 3 4 2	6
1 4 3 2	3
2 1 3 4	3
2 1 4 3	6
2 3 1 4	3
2 3 4 1	6
2 4 3 1	2
3 2 1 4	6
3 2 4 1	3
3 4 2 1	3
4 3 2 1	6

5.2. Rotations of triangulations

In this subsection, we describe a counterclockwise rotation of the $(n + 2)$-gon through an angle of $2\pi/(n + 2)$ as a geodesic path in the flip graph. We refer to any triangle with edges made up solely of diagonals $D_{i,i+j}$ for $j \geq 2$ as an internal triangle, and we denote the number of internal triangles in a triangulation $\mathcal{T}_\sigma$ by t_σ.

We will say that a diagonal $D_{i,j}$ is (counter)clockwise to another diagonal $D_{i,j'}$ if the vertex j is (counter)clockwise to j'. Similarly, $D_{i,j}$ is (counter)clockwise to $D_{i',j}$ if i is (counter)clockwise to i'. Given a triangulation $\mathcal{T}_\sigma$, the following algorithm describes a sequence of $n - 1 + t_\sigma$ edge flips that produce a rotation of $\mathcal{T}_\sigma$ by $2\pi/(n + 2)$ radians in the counterclockwise direction.

(1) For any diagonals $D_{i,j}$ with no incident diagonal counterclockwise to it, perform an edge flip at $D_{i,j}$ to get $D_{i-1,j-1}$. Continue to flip any such diagonals not previously flipped until no such diagonals remain.

(2) Choose an internal triangle T with a diagonal $D_{i,j}$ not previously flipped and admitting no incident diagonal $D_{i',j}$ counterclockwise to it.
Perform an edge flip at $D_{i,j}$ and then flip any diagonals not previously flipped that have no incident counterclockwise diagonals.

(3) If a diagonal $D_{i',j'}$ of T does have incident counterclockwise diagonals, then perform an edge flip at the counterclockwise-most of these incident diagonals. Flip any diagonals not previously flipped that now admit no incident counterclockwise diagonals.

(4) Repeat Step (3) until no diagonals counterclockwise to $D_{i',j'}$ remain. Perform an edge flip at $D_{i',j'}$. Once the second and third diagonals of T have been flipped, perform an edge flip at the initial diagonal previously belonging to T.

(5) Repeat Steps (3) and (4) starting with the remaining diagonals in the triangle corresponding to the counterclockwise diagonal flipped in Step (3). Continue until all possible diagonals have been flipped at.
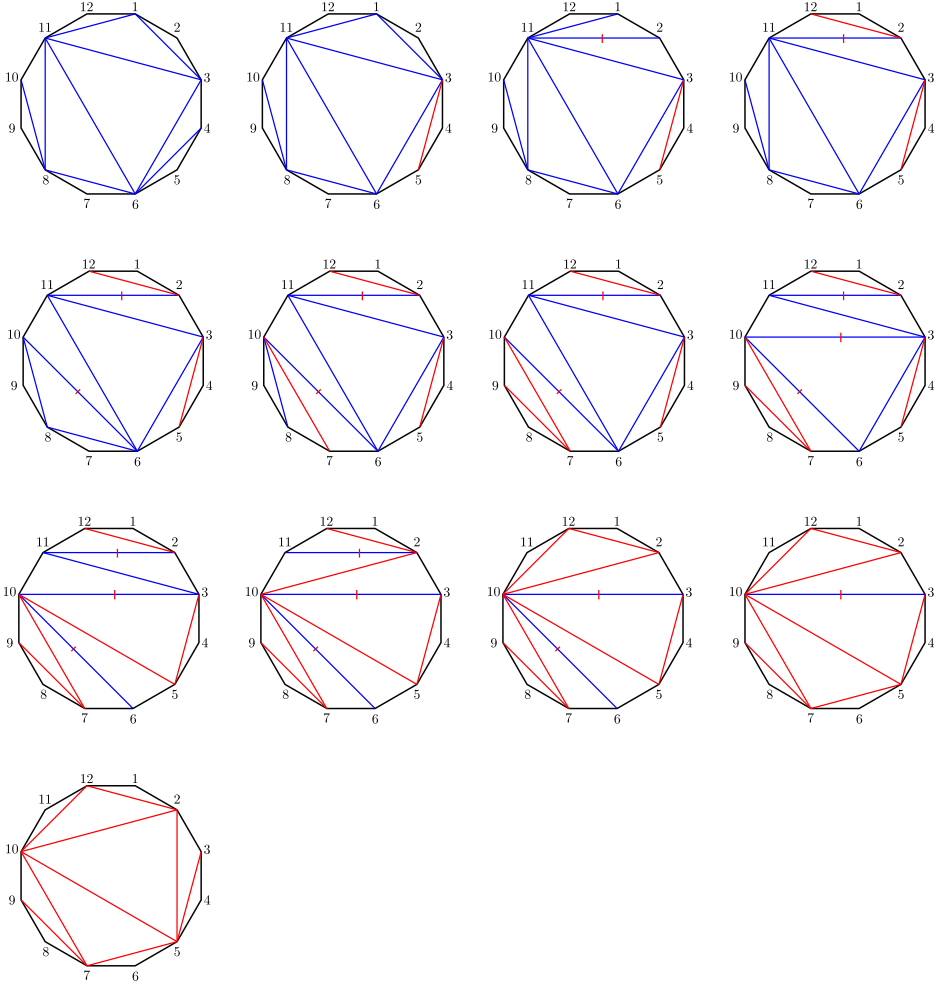
Figure 16. Counterclockwise rotation of a triangulation of the dodecagon by $10 - 1 + 3 = 12$ edge flips. The red diagonals are diagonals of the rotated triangulation, while the blue diagonals with a red mark are diagonals that are the result of a previous edge flip but are not diagonals of the rotated triangulation.

Example. If the triangulation $\mathcal{T}_\sigma$ only contains diagonals of the form $D_{i,j_1}, \ldots, D_{i,j_{n-1}}$, then the instructions above reduce to simply performing edge flips in reverse order of indexing, starting with $D_{i,j_{n-1}}$ and ending with D_{i,j_1}. See Figure 16 for a more involved example with three internal triangles.

Remark (Added in proof). While revising this manuscript, the author discovered that Theorem 5.6 below appeared previously in work of Cormier, Dillery, Resh, Serhiyenko, and Whelan in the context of automorphisms of cluster algebras and quiver combinatorics. The argument below was written without knowledge of their work but follows a similar line of reasoning. The interested reader is referred to their paper [14] for a more detailed discussion of the topic phrased in terms of maximal green sequences of cluster algebras.

Theorem 5.6 (Theorem 1.1 in [14]). *The number of edge flips required to realize a counterclockwise rotation of a triangulation $\mathcal{T}_\sigma$ of the $(n+2)$-gon by $2\pi/(n+2)$ is $n-1+t_\sigma$. The above instructions describe a sequence of $n-1+t_\sigma$ edge flips realizing such a rotation.*

Proof. We first argue that the number of flips needed to rotate a triangulation is at least $n-1+t_\sigma$. Since no diagonal of our original triangulation is a diagonal of our rotated triangulation, a rotation of the triangulation $\mathcal{T}_\sigma$ requires at least $n-1$ edge flips, i.e., as many edge flips as diagonals of $\mathcal{T}_\sigma$. However, in an internal triangle, it is not possible to apply a single edge flip to any of the three sides (or any other diagonal) so that the result is a side of the rotated triangle, or indeed any diagonal of the rotated triangulation. This is because each of the three sides prevents the side immediately counterclockwise to it from rotating in a counterclockwise direction. If none of the internal triangles share a side, then the claim follows. Otherwise, we argue that any two triangles sharing an edge still require at least two extra edge flips to rotate. The only possible way we could have fewer is if we could perform an edge flip at the shared side and then rotate the two triangles with a single edge flip of each of the remaining sides. However, if we apply an edge flip at the shared side, then the remaining sides of the two triangles prevent the opposite pair from achieving the desired rotation. Therefore, we must have at least $n-1+t_\sigma$ edge flips for a rotation of $2\pi/(n+2)$.

The algorithm given above describes a path in the flip graph of length $n-1+t_\sigma$ since we have two edge flips for a single diagonal in each internal triangle and one for every other diagonal. It remains to show that the result is a rotation of the initial triangulation $\mathcal{T}_\sigma$. In Step (1), an edge flip at a diagonal $D_{i,j}$ results in the diagonal $D_{i-1,j-1}$ precisely because there are no diagonals counterclockwise to it and therefore $D_{i,j}$ is a diagonal of the quadrilateral with sides $D_{i,j-1}, D_{j-1,j}, D_{i-1,j}, D_{i-1,i}$. It follows that each edge flip in Step (1) results in a diagonal of the rotated triangulation. If the triangulation $\mathcal{T}_\sigma$ has no internal triangles, then applying Step (1) to each of the $n-1$ diagonals results in the desired rotation.

Suppose that $\mathcal{T}_\sigma$ has at least one internal triangle. In Step (2), an edge flip at the diagonal $D_{i,j}$ in an internal triangle $\{D_{i,j}, D_{j,k}, D_{i,k}\}$ with no diagonal counterclockwise to it, results in the diagonal $D_{j-1,k}$. Once the remaining diagonals of the triangle have no incident counterclockwise diagonals, Step (4) applies an edge flip to them so that $D_{i,k}$ becomes $D_{i-1,j-1}$ and $D_{j,k}$ becomes $D_{j-1,k-1}$. Step (4) then flips $D_{j-1,k}$ to $D_{i-1,k-1}$. Crucially, the order of edge flips ensures that during Steps (2)-(4), we strictly decrease the number of counterclockwise incident diagonals to $D_{j,k}$ and $D_{i,k}$ at each step. After rotating our initial triangle, we can continue this process with the next internal triangle.

It remains to show that in Step (2), a diagonal $D_{i,j}$ of an internal triangle with no incident counterclockwise diagonals $D_{i',j}$ always exists. If $D_{i,j}$ has an incident counter-

clockwise diagonal not belonging to an internal triangle, then Step (1) will apply an edge flip at such a diagonal so that it is no longer counterclockwise to $D_{i,j}$. If $D_{i,j}$ has an incident counterclockwise diagonal that belongs to an internal triangle, then there is some counterclockwise-most diagonal $D_{i,j'}$ also belonging to an internal triangle. Note that an edge flip at $D_{i,j'}$ removes one of the diagonals counterclockwise to $D_{i,j}$, so we can repeat this argument until we have performed an edge flip at all such diagonals. ∎

Remark. For triangulations that allow for a choice of ordering edge flips, it follows from a theorem of Pournin (see Theorem 2 in [32]) that naively proceeding with any of the equivalent options will still yield a geodesic. We can reinterpret this in the cluster algebraic setting as the fact that distant mutations commute. In this context, any geodesic path gives the mutations describing the cluster automorphism induced by the Kálmán loop.

5.3. Edge flips in terms of permutations

In this subsection, we describe an edge flip at a diagonal $D_{j,l}$ of the triangulation $\mathcal{T}_\sigma$ in terms of the 312-avoiding permutation σ.

Let $\sigma \in S_n$ be a 312-avoiding permutation with corresponding triangulation given by the clip sequence bijection. Consider a quadrilateral with sides $D_{i,j}$, $D_{j,k}$, $D_{k,l}$ and $D_{i,l}$ appearing in the triangulation $\mathcal{T}_\sigma$. Figure 17 depicts this quadrilateral with two possible diagonals, $D_{i,k}$ and $D_{j,l}$ separating it into two triangles. An edge flip at one of these diagonals yields the other.
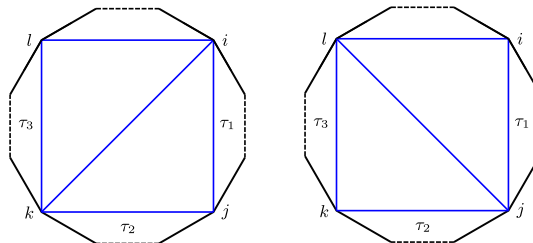
Figure 17. Schematic of an edge flip depicting the triangulation $\mathcal{T}_\sigma$ (left) and the result of applying an edge flip to $\mathcal{T}_\sigma$ at $D_{i,k}$ (right). The dotted lines represent arbitrarily many edges of the $(n+2)$-gon and the indices are chosen so that either $1 \le i < j < k < l \le n+1$ or $j < k < l = n+1, i = n+2$. The labels $\tau_1, \tau_2,$ and τ_3 represent subwords of σ corresponding to different section of $\mathcal{T}_\sigma$. If any of the edges of the quadrilateral lie on the $(n+2)$-gon, then we consider the corresponding τ_i to be the empty word.

As in the orbit size algorithm, we can determine the structure of σ based on the existence of the edges of the quadrilateral. Specifically, σ admits the subwords $\tau_1, \tau_2,$ and τ_3, where the subword τ_1 contains the letters $i+1, \ldots, j-1$, the subword τ_2 contains the letters $j+1$ and $k-1$, and the subword τ_3 contains the letters $k+1, \ldots, l-1$. From this construction, we can deduce the effect on σ of a single edge flip at $D_{i,j}$.

Theorem 5.7. *Given a triangulation $\mathcal{T}_\sigma$ containing a quadrilateral $ijkl$ with diagonal $D_{i,k}$, the 312-avoiding permutation σ is of the form $\ldots \tau_1 \tau_2 j \tau_3 k \ldots$ An edge flip at the diagonal $D_{i,k}$ yields a permutation of the form $\ldots \tau_1 \tau_2 \tau_3 k j \ldots$*

Proof. The theorem follows from the observation that each τ_i must contain at least one ear (that is, a triangle of with edges $D_{i,i+1}$, $D_{i,i+2}$ and $D_{i+1,i+2}$) of the triangulation $\mathcal{T}_\sigma$. Therefore, under the clip sequence bijection, the word τ_i appears before τ_j if $i < j$. Moreover, the vertex labels j, k appear only after the two quadrants immediately adjacent to the vertex have been deleted under the clip sequence process. Thus, the two 312-avoiding permutations corresponding to the triangulation $\mathcal{T}_\sigma$ and the triangulation resulting from applying an edge flip are precisely of the form described. ∎

Example. Consider the permutation $\sigma = 154362$. If we wish to apply an edge flip to the diagonal $D_{2,6}$, then we can identify the vertex labels of the relevant quadrilateral as $i = 2, j = 3, k = 6$, and $l = 7$. This immediately tells us that τ_1 and τ_3 are both empty and τ_2 is the subword 54. Therefore, Theorem 5.7 above implies that we simply interchange j and k to get the resulting permutation $\mu(\sigma) = 154632$. See Figure 18 for the triangulations $\mathcal{T}_\sigma$ and the triangulation resulting from the edge flip.
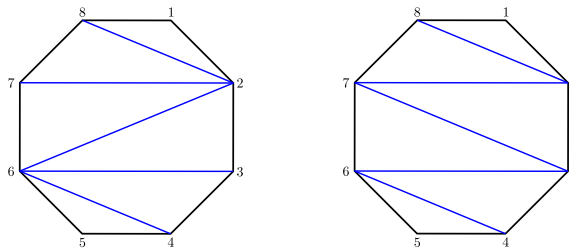
Figure 18. An edge flip at the diagonal $D_{2,6}$ in the triangulation $\mathcal{T}_{154362}$ yields the permutation 154632.

Together with Theorem 5.6, the above computation gives an explicit combinatorial construction of Kálmán loop in terms of geodesics paths of the flip graph and the corresponding behavior of 312-avoiding permutations.

References

[1] Arnol'd, V. I.: *Singularities of caustics and wave fronts*. Math. Appl. (Soviet Ser.) 62, Kluwer Academic Publishers Group, Dordrecht, 1990.

[2] Arnol'd, V. I. and Givental, A. B.: Symplectic geometry. In *Dynamical systems, IV*, pp. 1–138. Encyclopaedia of Mathematical Sciences 4, Springer, Berlin, 2001

[3] Assem, I., Schiffler, R. and Shramchenko, V.: Cluster automorphisms. *Proc. Lond. Math. Soc. (3)* **104** (2012), no. 6, 1271–1302.

[4] Bourgeois, F., Sabloff, J. M. and Traynor, L.: Lagrangian cobordisms via generating families: construction and geography. *Algebr. Geom. Topol.* **15** (2015), no. 4, 2439–2477.

[5] Casals, R.: Lagrangian skeleta and plane curve singularities. *J. Fixed Point Theory Appl.* **24** (2022), no. 2, article no. 34, 43 pp.

[6] Casals, R. and Gao, H.: Infinitely many Lagrangian fillings. *Ann. of Math. (2)* **195** (2022), no. 1, 207–249.

[7] Casals, R., Gorsky, E., Gorsky, M., Le, I., Shen, L. and Simental, J.: Cluster structures on braid varieties. Preprint 2022, arXiv: 2207.11607.

[8] Casals, R., Gorsky, E., Gorsky, M. and Simental, J.: Algebraic weaves and braid varieties. Preprint 2020, arXiv: 2012.06931.

[9] Casals, R. and Ng, L.: Braid loops with infinite monodromy on the Legendrian contact DGA. *J. Topol.* **15** (2022), no. 4, 1927–2016.

[10] Casals, R. and Weng, D.: Microlocal theory of Legendrian links and cluster algebras. Preprint 2022, arXiv: 2204.13244.

[11] Casals, R. and Zaslow, E.: Legendrian weaves: N-graph calculus, flag moduli and applications. *Geom. Topol.* **26** (2022), no. 8, 3589–3745.

[12] Chantraine, B.: Lagrangian concordance of Legendrian knots. *Algebr. Geom. Topol.* **10** (2010), no. 1, 63–85.

[13] Chekanov, Y.: Differential algebra of Legendrian links. *Invent. Math.* **150** (2002), no. 3, 441–483.

[14] Cormier, E., Dillery, P., Resh, J., Serhiyenko, K. and Whelan, J.: Minimal length maximal green sequences and triangulations of polygons. *J. Algebraic Combin.* **44** (2016), no. 4, 905–930.

[15] Ekholm, T., Honda, K. and Kámán, T.: Legendrian knots and exact Lagrangian cobordisms. *J. Eur. Math. Soc. (JEMS)* **18** (2016), no. 11, 2627–2689.

[16] Eliashberg, Y. and Polterovich, L.: Local Lagrangian 2-knots are trivial. *Ann. of Math. (2)* **144** (1996), no. 1, 61–76.

[17] Etnyre, J. and Ng, L.: Legendrian contact homology in $\mathbb{R}^3$. In *Surveys in differential geometry 2020. Surveys in 3-manifold topology and geometry*, pp. 103–161. Surv. Differ. Geom. 25, International Press, Boston, MA, 2022.

[18] Euler, L.: Specimen algorithmi singularis. *Novi Commentarii Academiae Scientiraum Petropolitanae* **9** (1764), 53–69.

[19] Fomin, S., Williams, L. and Zelevinsky, A.: Introduction to cluster algebras: Chapters 1-3. Preprint 2020, arXiv: 1608.05735, v3.

[20] Fomin, S., Williams, L. and Zelevinsky, A.: Introduction to cluster algebras: Chapters 4-5. Preprint 2020, arXiv: 1707.07190, v2.

[21] Fomin, S. and Zelevinsky, A. Cluster algebras. II. Finite type classification. *Invent. Math.* **154** (2003), no. 1, 63–121.

[22] Frame, J.: Continued fractions and matrices. *Amer. Math. Monthly* **56** (1949), no. 2, 98–103.

[23] Gao, H., Shen, L. and Weng, D.: Augmentations, fillings, and clusters. Preprint 2020, arXiv: 2008.10793.

[24] Geiges, H.: *An introduction to contact topology*. Cambridge Stud. Adv. Math. 109, Cambridge University Press, Cambridge, 2008.

[25] Hughes, J.: Weave realizability for D-type. *Algebr. Geom. Topol.* **23** (2023), 2735–2776.

[26] Kálmán, T.: Contact homology and one parameter families of Legendrian knots. *Geom. Topol.* **9** (2005), 2013–2078.

[27] Kálmán, T.: Braid-positive Legendrian links. *Int. Math. Res. Not.* (2006), article no. 14874, 29 pp.

[28] Karlsson, C.: A note on coherent orientations for exact Lagrangian cobordisms. *Quantum Topol.* **11** (2020), no. 1, 1–54.

[29] Ng, L. L.: Computable Legendrian invariants. *Topology* **42** (2003), no. 1, 55–82.

[30] Pan, Y.: Exact Lagrangian fillings of Legendrian $(2, n)$ torus links. *Pacific J. Math.* **289** (2017), no. 2, 417–441.

[31] Oh, Y.-G.: *Symplectic topology and Floer homology. Vol. 1. Symplectic geometry and pseudo-holomorphic curves*. New Math. Monogr. 28, Cambridge University Press, Cambridge, 2015.

[32] Pournin, L.: The diameter of associahedra. *Adv. Math.* **259** (2014), 13–42.

[33] Regev, A.: A bijection between triangulations and 312-avoiding permutations. Preprint 2013, arXiv: 1311.1955.

[34] Sleator, D. D., Tarjan, R. E. and Thurston, W. P.: Rotation distance, triangulations, and hyperbolic geometry. *J. Amer. Math. Soc.* **1** (1988), no. 3, 647–681.

[35] Shende, V., Treumann, D., Williams, H. and Zaslow, E.: Cluster varieties from Legendrian knots. *Duke Math. J.* **168** (2019), no. 15, 2801–2871.

[36] Shende, V., Treumann, D. and Zaslow, E.: Legendrian knots and constructible sheaves. *Invent. Math.* **207** (2017), no. 3, 1031–1133.

[37] Treumann, D. and Zaslow, E.: Cubic planar graphs and Legendrian surface theory. *Adv. Theor. Math. Phys.* **22** (2018), no. 5, 1289–1345.

[38] Ustinov, A.: A short proof of Euler's identity for continuants. *Mat. Zametki* **79** (2006), no. 1, 155–156; translation in *Math. Notes* **79** (2006), no. 1-2, 146–147.

James Hughes
Department of Mathematics, University of California Davis,
Shields Avenue, Davis, CA 95616, USA;
jmhughes@math.ucdavis.edu